

Randomized Spectral Clustering in Large-Scale Stochastic Block Models

Hai Zhang[†], Xiao Guo^{†*}, Xiangyu Chang[‡]

[†] School of Mathematics, Northwest University, China

[‡] School of Management, Xi'an Jiaotong University, China

July 15, 2022

Abstract

Spectral clustering has been one of the widely used methods for community detection in networks. However, large-scale networks bring computational challenge to it. In this paper, we study spectral clustering using randomized sketching algorithms from a statistical perspective, where we typically assume the network data are generated from a stochastic block model. To do this, we first use the recent developed sketching algorithms to derive two randomized spectral clustering algorithms, namely, the random projection-based and the random sampling-based spectral clustering. Then we study the theoretical bounds of the resulting algorithms in terms of the approximation error for the population adjacency matrix, the misclustering error, and the estimation error for the link probability matrix. It turns out that, under mild conditions, the randomized spectral clustering algorithms perform similarly to the original one. We also conduct numerical experiments to support the theoretical findings.

Keywords: Network, Community detection, Random projection, Random sampling

*Xiao Guo is the corresponding author and the authors gratefully acknowledge the supporting of National Natural Science Foundation of China (NSFC, 11571011, 11771012, 61502342 and U1811461).

1 Introduction

Extraordinary amounts of data are being collected in the form of arrays across many scientific domains, including sociology, physics, and biology, among others. In particular, network data and network data analysis have received a lot of attention because of their wide-ranging applications in these areas (Newman, 2018; Goldenberg et al., 2010; Kolaczyk, 2009). Community detection is one of the fundamental problems in network analysis, where the goal is to find groups of nodes that are, in some sense, more similar to each other than to the other nodes. Past decades have seen various procedures on community detection including modularity maximization, spectral clustering, likelihood methods, semidefinite programming, among others; see Abbe (2018) for a recent survey. However, large networks, namely, networks with various nodes or edges, bring great challenge to these community detection procedures despite the increasing computational power. Taking the spectral clustering that we will focus on in this paper as an example, the eigenvalue decomposition therein is time demanding when the dimension becomes large.

Randomization has become one popular method for modern large-scale data analysis; see Mahoney (2011), and Drineas and Mahoney (2016), and references therein. The general idea is that, depending on the problem of interest, one use a degree of randomness to construct a small “sketch” of the full data set, and then use the resulting sketched data instead to reduce the computational burden. Random projection and random sampling are the two general approaches to obtain such a sketch matrix. Roughly speaking, random projection reduces the computational cost by projecting the data matrix to a small dimensional space in order to approximate the data. While random sampling algorithms lighten the computational burden by sampling and rescaling the data in some manner. The randomization techniques have been applied to the least square regression (Drineas et al., 2006, 2011, 2012), and the low-rank matrix approximation (Halko et al., 2011; Martinsson, 2016; Witten and Candès, 2015; Mahoney and Drineas, 2009), among many others. Most works in this area were analyzed from an algorithmic perspective, where the randomized algorithm could lead to approximately as good performance as the full data at hand does for some problems of interest. However, from a statistical perspective, our aim is not only

to derive randomized algorithms which perform well on a particular data set, but also to understand how well they perform under some underlying mechanisms. In the context of regression, there have been a few works that study the randomized algorithms under underlying regression models—for example, the ordinary linear regression (Ma et al., 2015; Raskutti and Mahoney, 2016; Wang et al., 2019), the logistic regression (Wang et al., 2018; Wang, 2018), the ridge regression (Wang et al., 2017), the constrained regressions (Pilanci and Wainwright, 2016, 2017), and the spatial autoregressive (SAR) models (Zhou et al., 2017; Li and Kang, 2019), among others. Just like they have studied how well the randomized algorithms can estimate the underlying regression model, it is natural and important to study how well we can use the randomization techniques to detect the communities in a “true” network model. The Stochastic block model (SBM) (Holland et al., 1983) is a simple but expressive network model that captures the community structure of networks observed in the real world. In a SBM, nodes are partitioned into several distinct communities, and conditioned on the underlying community assignments, the edges are generated independently according to the community membership of their end nodes. Nodes within the same community are generally more likely to be connected than the other nodes. The SBM is popular among statisticians because it can be rigorously studied coupling with various network community detection procedures; see Abbe (2018) for an excellent review.

In this work, we focus on studying how randomization can be used to reduce the computational cost of the spectral clustering, and on understanding how well the resulting randomized spectral clustering algorithms perform under the stochastic block models. Spectral clustering is a popular and simple algorithm for clustering which consists of the following two steps. One first conducts the eigenvalue decomposition of the adjacency matrix or the laplacian matrix, and then runs the k -means on several leading eigenvectors to obtain the nodes clusters or communities (Von Luxburg, 2007). It is well known that the first step of spectral clustering generally requires $O(n^3)$ time where n denotes the number of nodes, which is time demanding when n becomes large. Regardless of the computational issues, it has been shown to enjoy good theoretical properties within the SBM framework; see, Rohe et al. (2011); Choi et al. (2012); Lei and Rinaldo (2015); Qin and Rohe (2013);

Sarkar et al. (2015); Joseph and Yu (2016); Su et al. (2017), among many others. Facing large networks, in this paper, we utilize the idea in randomization to derive two kinds of randomized spectral clustering algorithms; namely, the random projection-based and the random sampling-based spectral clustering, and in particular we study their theoretical properties under the SBM. We focus on the adjacency matrix A of the network. The random projection-based method is motivated as follows. Note that the adjacency matrix inherits a low-rank structure naturally since it is sampled from a SBM. Therefore, if one can make use of such low-rank structure to derive a matrix with lower dimension which captures the essential information of A , then the eigenvalue decomposition of this matrix can help to derive that of A , which in turn reduces the computational cost. Indeed, the recently developed randomized low-rank matrix approximation algorithms provide a powerful tool for performing such low-rank matrix approximation (Halko et al., 2011; Witten and Candès, 2015; Martinsson, 2016). Specifically, these techniques utilize some amount of randomness to compress the columns and rows of A to l ($l \ll n$) linear combinations of the columns and rows of A . The eigenvalue decomposition on the resulting l -dimensional matrix can be largely reduced since l is far smaller than n . The random projection-based spectral clustering refers to the original spectral clustering with its first step replaced by the randomized eigenvalue decomposition. On the other hand, the computational cost of the original spectral clustering can be reduced via the random sampling. Note that we only need to find a few leading eigenvectors of A , which can be obtained using many fast iterative methods, such as orthogonal iteration and Lanczos iteration. And it is well known that the time complexity of iterative algorithms is the number of non-zero elements of A multiplied by the number of iterations. Therefore, if we sample the elements of A in some way to obtain a sparser matrix, then the time for computing its leading eigenvectors will be largely reduced. There have been a few works on the randomized matrix sparsification; see Gittens and Tropp (2009); Achlioptas and McSherry (2007); Arora et al. (2006); Li et al. (2016), among others. In particular, Li et al. (2016) apply the sampling technique to study the network cross-validation problem. In this work, we use a simple sampling strategy to obtain a sparsified matrix; that is, sample each pair of nodes with equal probability,

then use the iteration method of [Baglama and Reichel \(2005\)](#) to find its leading vectors, and after that perform the k -means algorithm on these eigenvectors, which we refer to the random sampling-based spectral clustering.

The contributions of the paper are as follows. We apply the random projection and random sampling schemes to the spectral clustering-based network community detection problem, and analyze their properties from a statistical perspective. Specifically, we theoretically justify them in terms of the approximation error that measures the derivation of the randomized matrix \tilde{A} of the adjacency matrix A from the population matrix P , and the error of misclustering. In addition, although the spectral clustering is nonparametric in nature, we develop a simple method to estimate the link probability matrix B based on the output clusters where B_{kl} is the edge probability between any node pairs in communities k and l , and provide its theoretical bound. Note that we focus on the weak consistency of the pure spectral clustering in SBMs, which to the best of our knowledge has been studied only by [Rohe et al. \(2011\)](#) and [Lei and Rinaldo \(2015\)](#). In particular, [Lei and Rinaldo \(2015\)](#) requires less condition on the graph sparsity. Hence, we compare our results with those in [Lei and Rinaldo \(2015\)](#). The theoretical bounds in a simplified case in terms of the aforementioned three aspects are summarized in [Table 1](#). It turns out that the proposed randomized spectral clustering algorithms perform comparably to the original spectral clustering. In particular, the approximation error bounds of the randomized spectral clustering algorithms are the same as the best known concentration bound of $\|A - P\|_2$ ([Lei and Rinaldo, 2015](#); [Chin et al., 2015](#); [Gao et al., 2017](#)), provided that the sampling rate in the random sampling scheme is fixed. The misclustering error bounds are optimal in the sense that there is no estimator which is weakly consistent when $n\alpha_n = O(1)$, and K and p are fixed, where K denotes the number of communities and α_n denotes the maximum probability of an edge. In addition, the link probability error bounds vanish under mild conditions, which has not been studied in most of the literature on the spectral clustering. Finally, the empirical results support our theoretical results.

The remainder of the paper is organized as follows. [Section 2](#) defines the notation and introduces the SBM and spectral clustering in more detail. [Section 3](#) includes the random

Table 1: A summary of the main results. The approximation error bounds, the misclustering error bounds, and the link probability error bounds of the random projection-based spectral clustering, the random sampling-based spectral clustering, and the original spectral clustering in [Lei and Rinaldo \(2015\)](#) are displayed. In this table, K is the number of true clusters, n is the network size, and p is the sampling rate in the random sampling scheme. The bounds are a simplified version of our results under the special case (4.5).

Bounds	Random projection	Random sampling	Original
Approximation error	$O_p(\sqrt{\log n})$ Theorem 1	$O_p(\frac{\sqrt{\log n}}{p})$ Theorem 4	$O_p(\sqrt{\log n})$
Misclustering error	$O_p(\frac{K^3}{\log n})$ Theorem 2	$O_p(\frac{K^3}{p^2 \cdot \log n})$ Theorem 5	$O_p(\frac{K^3}{\log n})$
Link probability error	$O_p(\frac{K^{3/2} \log n}{n})$ Theorem 3	$O_p(\max\{\frac{K^{3/2} \sqrt{\log n}}{np}, \frac{K^{3/2} \log n}{n}\})$ Theorem 6	-

projection-based and random sampling-based spectral clustering schemes that we consider. Section 4 presents the theoretical results. Section 5 and 6 include the simulation and real experiments that verify the theoretical results and show the effectiveness of the proposed methods. Section 7 concludes with discussion. Proofs are provided in the appendix.

2 Preliminaries

In this section, we provide some notation and briefly introduce the stochastic block model and the spectral clustering algorithm. In particular, the rationality of spectral clustering under stochastic block models is discussed.

2.1 Notation

Let $\mathbb{M}_{n,K}$ be the set of all $n \times K$ matrices that have exactly one 1 and $K - 1$ 0's in each row. Any $\Theta \in \mathbb{M}_{n,K}$ is called a *membership matrix* where each row represents the community membership of a node; for example, node i belongs to community $g_i \in \{1, \dots, K\}$ if and only

if $\Theta_{ig_i} = 1$. For $1 \leq k \leq K$, let $G_k = G_k(\Theta) = \{1 \leq i \leq n : g_i = k\}$, which consists of nodes with their community membership being k , and let $n_k = |G_k|$. For any matrix $A_{n \times n}$ and $I, J \subseteq [n]$, A_{I*} and A_{*J} denote the submatrix of A consisting of the corresponding rows and columns, respectively. $\|A\|_F$ and $\|A\|_\infty$ denote the Frobenius norm and the element-wise maximum absolute value of A , respectively. And $\|A\|_{2,\infty} = \max_i (\sum_j A_{ij}^2)^{1/2}$. We use $\|\cdot\|_2$ to denote the Euclidean norm of a vector and the spectral norm of a matrix. In addition, $\text{diag}(A)$ denotes the matrix with its diagonal elements being the same as those of A and non-diagonal elements being 0's.

2.2 Stochastic block model

The stochastic block model (SBM) introduced by [Holland et al. \(1983\)](#) is a class of probabilistic model for networks with well-defined communities. For a potential network with n nodes and K communities, the model is parameterized by the membership matrix $\Theta \in \mathbb{M}_{n,K}$, and the connectivity matrix $B \in [0, 1]^{K \times K}$ where B is of full rank, symmetric, and the entry of B ; for example, B_{kl} , represents the edge probability between any node in community l and any node in community k . Given Θ and B , the network adjacency matrix $A = (a_{ij})_{1 \leq i, j \leq n} \in \{0, 1\}^{n \times n}$ is generated as

$$a_{ij} = \begin{cases} \text{Bernoulli}(B_{g_i g_j}) & \text{if } i < j, \\ 0, & \text{if } i = j, \\ a_{ij}, & \text{if } i > j. \end{cases} \quad (2.1)$$

Define $P = \Theta B \Theta^\top$, then it is easy to see that P is the population version of A in the sense that $\mathbb{E}(A) = P - \text{diag}(P)$. Under the SBMs, the goal of community detection is to use the adjacency matrix A to recover the membership matrix Θ up to column permutations. In this paper, we focus on the spectral clustering.

2.3 Spectral clustering

Spectral clustering is a popular and simple algorithm for community detection in networks (Von Luxburg, 2007). It generally consists of two steps. The first step is to perform the eigenvalue decomposition of a suitable matrix representing the network, where we consider the simple adjacency matrix A , and then put the eigenvectors of A corresponding to the K largest eigenvalues into a $n \times K$ matrix \hat{U} . The next step is treat each row of \hat{U} as a point in \mathbb{R}^K and run k -means on \hat{U} with K clusters. In this paper, for simplicity, we use the standard and efficient heuristic Lloyd’s algorithm. The resulting clustering labels are arranged as $\hat{\Theta} \in \mathbb{M}_{n,K}$, and the K -dimensional centroid vectors are collected as $\hat{X} \in \mathbb{R}^{K \times K}$, where the i th row of \hat{X} corresponds to the centroid of the i th cluster. We summarize the spectral clustering in Algorithm 1.

The spectral clustering is very interpretable in SBMs because P , the population version of A , has eigenvectors that reveal the true clusters. In other words, the eigenvectors of P have K distinct rows, and two rows are identical if and only if the corresponding nodes are in the same community (Lei and Rinaldo, 2015; Rohe et al., 2011). For ease of reference, we reproduce the Lemma 2.1 of Lei and Rinaldo (2015) as follows.

Lemma 1 *For a SBM with K communities parametrized by (Θ, B) where B is of full rank, suppose $P = U\Sigma U^\top$ is the eigenvalue decomposition of $P = \Theta B \Theta^\top$, then $U = \Theta X$ where $X \in \mathbb{R}^{K \times K}$ is of full rank and $\|X_{k*} - X_{l*}\|_2 = \sqrt{n_k^{-1} + n_l^{-1}}$.*

By Lemma 1, we can imagine that the spectral clustering would cluster well if the K leading eigenvectors of A are close to those of the population P , which can be achieved if A is close to P in some sense under the rationality of the Davis-Kahan theorem (Davis and Kahan, 1970). We will explain that formally in the theoretical part.

It is well known that the eigenvalue decomposition in the spectral clustering is time consuming when the number of nodes n is large, thus how to improve its efficiency without sacrificing much community detection accuracy in the context of SBMs is of great importance. In the following sections, we will make use of the recently developed randomization techniques—namely, the random projection and the random sampling, to try to answer this question. As will be seen later, these two strategies improve the computational efficiency of

the eigendecomposition by finding a randomized low-rank approximation of A in different ways. Specifically, the random projection scheme projects the rows and columns of A into a low-dimensional space. The time of A 's eigendecomposition will be largely shortened if one does it on the resulting smaller matrix and then post processes it to obtain the approximate eigenvector of A . While the random sampling scheme samples the node pairs of A to obtain a sparsified matrix, and then uses fast iterative methods to find leading eigenvectors of the resulting sparsified matrix. The procedure is not time consuming since the time complexity of iterative methods is proportional to the number of non-zero elements. In Section 3, we will introduce these two paradigms in more detail.

Algorithm 1 Spectral clustering for k clusters

Input:

Cluster number K , the adjacency matrix $A \in \mathbb{R}^{n \times n}$ of the network;

Output:

Estimated membership matrix $\hat{\Theta} \in \mathbb{M}_{n,K}$ and centroids $\hat{X} \in \mathbb{R}_{K \times K}$;

Estimated eigenvectors $\hat{U} = \hat{\Theta}\hat{X}$;

- 1: Find the K leading eigenvectors \hat{U} of A corresponding to the K largest eigenvalues of A .
 - 2: Treat each row of \hat{U} as a point in \mathbb{R}^K and run the Lloyd's algorithm on these points with K clusters. Let $(\hat{\Theta}, \hat{X})$ be the solution.
-

3 Randomized spectral clustering

In this section, we use the randomization techniques to derive two kinds of randomized spectral clustering—namely, randomized spectral clustering via random projection and random sampling.

3.1 Randomized spectral clustering via random projection

As mentioned earlier, the eigenvalue decomposition of A is computationally inefficient when the dimension of A becomes large. Recall that A is generated from a low-rank matrix $P = \Theta B \Theta^\top$, hence A inherits a low-rank structure naturally. Therefore, if one can make use

of such low-rank structure to derive a smaller matrix that captures the essential information of A , then the eigenvalue decomposition of the smaller matrix can help to derive that of A , which in turn reduces the computational cost. Fortunately, the randomization is a powerful tool for performing such low-rank matrix approximation (Halko et al., 2011; Witten and Candès, 2015; Martinsson, 2016). These techniques utilize some amounts of randomness to compress the input matrix to obtain a low-rank factorization efficiently, and we call this *random projection*. In this section, we introduce the random projection strategy in the context of eigenvalue decomposition.

Let us see how the random projection can help reduce the time for the eigenvalue decomposition of adjacency matrix A . For a symmetric matrix $A \in \mathbb{R}^{n \times n}$ with target rank K , we aim to find a orthonormal basis $Q \in \mathbb{R}^{n \times K}$ ($K \leq n$) such that

$$A \approx QQ^T A QQ^T \equiv \tilde{A}^{\text{rp}},$$

where \tilde{A}^{rp} is essentially a low-rank approximation of A . Before constructing Q , we here provide some insights. $Q \in \mathbb{R}^{n \times K}$ can be thought as a low-rank approximation of the column (row) space of matrix A . To see this, suppose the eigendecomposition of A is $A = \hat{U}_{n \times m} \hat{\Sigma}_{m \times m} \hat{U}_{m \times n}^T$, where m is the rank of A and \hat{U} represents the column (row) space of A . Then, when $Q = U$ and $m = K$, it is straightforward to see $A = QQ^T A QQ^T$. In addition, QQ^T is a projection operator which projects any vector $x \in \mathbb{R}^n$ to the column space of Q , i.e., $\|x - QQ^T x\|_2^2 = \min_{y \in \mathbb{R}^K} \|x - Qy\|_2^2$. Now let us see how to construct Q to approximate the column (row) space of A . Halko et al. (2011) build Q randomly by the following steps:

Step 1: Draw K n -dimensional random vectors $\{\omega_i\}_{i=1}^K$ independently from a distribution. Denote the random test matrix $\Omega = (\omega_1, \dots, \omega_K) \in \mathbb{R}^{n \times K}$.

Step 2: Form $y_i := A\omega_i$ for $i = 1, \dots, K$, where y_i 's are the independently weighted linear combinations of the columns of A . Denote the sketch matrix $Y = (y_1, \dots, y_K) = A\Omega \in \mathbb{R}^{n \times K}$.

Step 3: Orthonormalize Y via the QR decomposition $Y = QR$, where Q is what we are seeking.

Once Q is obtained, we can perform the eigenvalue decomposition on the smaller matrix $C := Q^T A Q \in \mathbb{R}^{K \times K}$, and then post process it to obtain the approximate eigenvectors of A , and finally perform the k -means clustering on these eigenvectors. In this way, the computational cost of the original spectral clustering is largely reduced. We call this procedure random projection-based spectral clustering.

The random test matrix Ω can be generated in various ways, specifically, the entries of can be i.i.d. standard gaussian, uniform, and rademacher distributions, among many others. In particular, for the gaussian test matrix, [Halko et al. \(2011\)](#) provide the probability bounds on the derivation of $QQ^T A$ from A conditional on A , which in turn ensures that \tilde{A}^{rp} and A are close by noting that,

$$\begin{aligned} \|A - \tilde{A}^{\text{rp}}\|_2 &= \|A - QQ^T A + QQ^T A - QQ^T A QQ^T\|_2 \\ &\leq \|A - QQ^T A\|_2 + \|QQ^T(A - A QQ^T)\|_2 \\ &\leq 2\|A - QQ^T A\|_2, \end{aligned} \tag{3.1}$$

where the last inequality holds due to the symmetry of A , $\|AB\|_2 \leq \|A\|_2 \|B\|_2$ for any matrices A and B , and $\|QQ^T\|_2 \leq 1$ which is implied by $(QQ^T)^2 = QQ^T$. In this paper, since A is not fixed but generated from a low-rank matrix P , we will actually use the bound of (3.1) with A replaced by P to derive the approximation bound $\|\tilde{A}^{\text{rp}} - P\|_2$, instead of combining $\|A - \tilde{A}^{\text{rp}}\|_2$ and $\|A - P\|_2$ straightforwardly to obtain the approximation bound.

The oversampling strategy is often used to improve the empirical performance of the randomized low-rank approximation ([Halko et al., 2011](#); [Witten and Candès, 2015](#); [Martinsson, 2016](#)). As most data matrices do not have exact rank K , it is desirable to use $l := K + r$ random projections instead of exact K projections to form the random sketch of A . In practice, $r = \{5, 10\}$ often suffices to get a good result ([Martinsson, 2016](#)).

Besides the oversampling scheme, the power iteration is another way to improve the quality of low-rank approximation. For some data matrices, the eigenvalues decay slowly that may lead to the information loss. Thus instead of forming the sketch Y on the basis of A , several authors incorporate q steps of a power iteration before constructing the sketch

matrix Y . Formally, it is defined as

$$Y := (AA^\top)^q A\Omega.$$

In practice, $q = 1$ or $q = 2$ is sufficient (Halko et al., 2011).

We summarize the random projection-based spectral clustering procedure with such power iteration and the aforementioned oversampling strategies in Algorithm 2.

Remark 1 *The time complexity of Algorithm 2 is dominated by the matrix multiplications when forming Y and C in step 2 and step 4, which take $O((2q + 1)n^2(K + r))$ and $O(n^2(K + r))$ time, respectively. In particular, the time complexity of step 2 can be improved to $O((2q + 1)n^2 \log(K + r))$ by using structured random test matrices, for example, the subsampled random Fourier transform (Halko et al., 2011; Erichson et al., 2019).*

Algorithm 2 Randomized spectral clustering via random projection

Input:

A target rank K , the adjacency matrix $A \in \mathbb{R}^{n \times n}$ of the network, an oversampling parameter r , and an exponent q ;

Output:

Membership matrix $\hat{\Theta}^{\text{rp}} \in \mathbb{M}_{n,K}$ and centroids $\hat{X}^{\text{rp}} \in \mathbb{R}^{K \times K}$;
 $\hat{U}^{\text{rp}} = \hat{\Theta}^{\text{rp}} \hat{X}^{\text{rp}}$;

- 1: Draw a $n \times (K + r)$ random test matrix Ω .
 - 2: Form the matrix $Y = (AA^\top)^q A\Omega$ by multiplying alternately with A and A^\top .
 - 3: Construct Q via orthonormalizing the columns of Y , i.e., $Y = QR$.
 - 4: Form $C = Q^\top A Q$ and denote $\tilde{A}^{\text{rp}} \equiv QCQ^\top$.
 - 5: Compute the eigenvalue decomposition of the small matrix: $C = U_s \Sigma_s U_s^\top$.
 - 6: Set \tilde{U}^{rp} to be the column subset of QU_s corresponding to the K largest values of Σ_s .
 - 7: Treat each row of \tilde{U}^{rp} as a point in \mathbb{R}^K and run the Lloyd's algorithm on these points with K clusters. Let $(\hat{\Theta}^{\text{rp}}, \hat{X}^{\text{rp}})$ be the solution.
-

3.2 Randomized spectral clustering via random sampling

Random projection methods reduce the computational burden by projecting the columns and rows of A onto a low-dimensional space using randomization techniques which results

in a small matrix being decomposed, thus speeding up the spectral clustering procedure. Another strategy is to do element-wise sampling from the adjacency matrix A , and then use fast iterative methods, say orthogonal iteration or Lanczos iteration, to find a nearly-optimal best rank K approximation of A . The motivation is that in spectral clustering, we aim to find the first K eigenvectors of A , or the best rank K approximation of A . And there exist many fast iterative methods for computing such low-rank matrix approximation; for example, orthogonal iteration and Lanczos iteration, of which the time complexity is the number of non-zero elements of A multiplied by the number of iterations. Hence, if we sample the elements of A in some way to obtain a sparser matrix, then the time for computing its rank K approximation will be largely reduced. In the meantime, we hope that the sampling scheme does not deteriorate the accuracy too much. In the sequel, we introduce the random sampling procedure and the corresponding randomized spectral clustering.

We adopt a simple sampling strategy to obtain a sparsified version of A . That is, randomly select each pair of the adjacency matrix A independently with probability p regardless of the value of A_{ij} , and the randomized sparsified matrix \tilde{A}^s is defined as

$$\tilde{A}_{ij}^s = \begin{cases} \frac{A_{ij}}{p}, & \text{if } (i, j) \text{ is selected,} \\ 0, & \text{if } (i, j) \text{ is not selected,} \end{cases}$$

for each $i < j$, and $\tilde{A}_{ji}^s = \tilde{A}_{ij}^s$ for each $i > j$. Once the sparsified matrix \tilde{A}^s is obtained, we can apply an iterative algorithm for the eigenvalue decomposition of \tilde{A}^s to attain the nearly-optimal rank K approximation of \tilde{A}^s such that

$$\tilde{A}^s \approx \tilde{U}_{n \times K}^{\text{rs}} \tilde{\Sigma}_{K \times K}^{\text{rs}} (\tilde{U}^{\text{rs}})_{K \times n}^{\text{T}} \equiv \tilde{A}^{\text{rs}}.$$

Then the Lloyd's algorithm can be applied on the rows of \tilde{U}^{rs} to find the clusters. Let $(\hat{\Theta}^{\text{rs}}, \hat{X}^{\text{rs}})$ be the solution. For reference, we summarize these steps in Algorithm 3.

Now we illustrate the steps in Algorithm 3 in more detail. There has been a few works on the randomized matrix sparsification; see [Achlioptas and McSherry \(2007\)](#); [Gittens](#)

and Tropp (2009); Spielman and Srivastava (2011), and references therein. In particular, Gittens and Tropp (2009) provide theoretical bounds on the approximation error of $\|\tilde{A}^s - A\|_2$ with respect to several norms, where A is assumed to be fixed. In our context, we are interested in how the sparsified and then low-rank approximated matrix \tilde{A}^{rs} performs under the SBMs, namely, the derivation of \tilde{A}^{rs} from P . We will actually make use of the low-rank nature of \tilde{A}^{rs} to derive the approximation bound $\|\tilde{A}^{\text{rs}} - P\|_2$. In addition, the selected elements of A in *Step 1* of Algorithm 3 are divided by p_s to ensure that $\mathbb{E}(A^s) = A$ conditioned on A .

Note that the past decades have seen fruitful work on the iterative algorithms for computing the low-rank approximation of the matrix; see Baglama and Reichel (2005); Allen-Zhu and Li (2016); Lehoucq (1995), among many others. In this paper, we use the method of Baglama and Reichel (2005) in *Step 2*. Specifically, we use the R package `irlba`. It should be noted that the iteration algorithms in *Step 2* yields the nearly-optimal solution instead of the exactly-optimal rank K approximation and it is acceptable to work with a nearly-optimal low-rank approximation. In the theoretical analysis, we treat *Step 2* as a black box and suppose the best rank K approximation is obtained. We mainly deal with approximation error induced by *Step 1*.

Algorithm 3 Randomized spectral clustering via random sampling

Input:

A target rank K , the adjacency matrix $A \in \mathbb{R}^{n \times n}$ of the network, a sampling probability p ;

Output:

Membership matrix $\hat{\Theta}^{\text{rs}} \in \mathbb{M}_{n,K}$ and centroids $\hat{X}^{\text{rs}} \in \mathbb{R}^{K \times K}$;
 $\hat{U}^{\text{rs}} = \hat{\Theta}^{\text{rs}} \hat{X}^{\text{rs}}$;

- 1: Randomly select each pair of the adjacency matrix A independently with probability p regardless of the value of A_{ij} , and for each pair $(i, j)(i < j)$, the symmetric sparsified matrix \tilde{A}^s is defined as $\tilde{A}_{ij}^s = \frac{A_{ij}}{p}$ if (i, j) is selected, and $\tilde{A}_{ij}^s = 0$ otherwise.
- 2: Apply an iterative algorithm to obtain the nearly-optimal rank K approximation of \tilde{A}^s such that

$$\tilde{A}^s \approx \tilde{U}_{n \times K}^{\text{rs}} \tilde{\Sigma}_{K \times K}^{\text{rs}} (\tilde{U}^{\text{rs}})_{K \times n}^{\top} \equiv \tilde{A}^{\text{rs}}.$$

- 3: Treat each row of \tilde{U}^{rs} as a point in \mathbb{R}^K and run the Lloyd's algorithm on these points with K clusters. Let $(\hat{\Theta}^{\text{rs}}, \hat{X}^{\text{rs}})$ be the solution.
-

4 Theoretical analysis

In this section, we theoretically justify the performance of two randomization schemes on spectral clustering under the model set-up of SBMs. Specifically, for each method, we evaluate its performance from the following three aspects. First, we derive an upper bound on how the randomized matrix \tilde{A}^{rp} (or \tilde{A}^{rs}) deviates from $P = \Theta B \Theta^\top$, the population adjacency matrix of SBM. Then, we use these results to bound the mis-clustered rate of the randomized spectral clustering algorithms. At last, we use the estimated clusters to obtain an estimate of B , and provide its theoretical bound.

4.1 Random projection

Recall that $\tilde{A}^{\text{rp}} = Q Q^\top A Q Q^\top$ is the randomized version of A via random projection, and $P = \Theta B \Theta^\top = \mathbb{E}(A) + \text{diag}(P)$ is the population of A except the diagonal elements. The following theorem gives the derivation of \tilde{A}^{rp} from P .

Theorem 1 *Let A be an $n \times n$ adjacency matrix generated from a stochastic block model (Θ, B) , and assume that the population adjacency matrix $P = \Theta B \Theta^\top$ is of rank K . Let $\tilde{A}^{\text{rp}} = Q Q^\top A Q Q^\top$ be the randomized approximation of A in Algorithm 2 where the target rank is K , $K + r \leq n$, and the test matrix Ω has i.i.d. standard gaussian entries. If*

$$\max_{kl} B_{kl} \leq \alpha_n \text{ for some } \alpha_n \geq c_0 \log n/n, \tag{A1}$$

then for any $s > 0$, there exists a constant $c_1 = c_1(s, c_0)$ such that

$$\|\tilde{A}^{\text{rp}} - P\|_2 \leq c_1 \sqrt{n \alpha_n}, \tag{4.1}$$

with probability at least $1 - n^{-s}$.

The proof of Theorem 1 can be found in the **Appendix**. (A1) is a weak condition on the population network sparsity, which requires the maximum expected node degree is of order $\log n$ or higher, which is used to obtain a sharp bound of $\|A - P\|_2$ (Lei and Rinaldo, 2015; Gao et al., 2017; Chin et al., 2015). Surprisingly, the bound in (4.1) is the same as the best

concentration bound of $\|A - P\|_2$ (Lei and Rinaldo, 2015; Chin et al., 2015; Gao et al., 2017), to the best of our knowledge. Thus in the sense of the spectral norm, the randomized matrix \tilde{A}^{rp} and the non-randomized matrix A behave the same if A is generated from a SBM, and the randomization pays no price. The reason for such results is that $\|\tilde{P}^{\text{rp}} - P\|_2$ is 0 with probability 1 under the condition in Theorem 1 (Halko et al., 2011), and thus the bound of $\|\tilde{A}^{\text{rp}} - P\|_2$ is dominated by that of $\|A - P\|_2$ by noting that

$$\begin{aligned}\|\tilde{A}^{\text{rp}} - P\|_2 &= \|QQ^\top AQQ^\top - P\|_2 = \|QQ^\top(A - P)QQ^\top + QQ^\top PQQ^\top - P\|_2 \\ &\leq_{a.s.} \|QQ^\top(A - P)QQ^\top\|_2 + 0 \leq \|A - P\|_2.\end{aligned}$$

With the derivation of \tilde{A}^{rp} from P at hand, we are ready to justify the clustering performance of Algorithm 2. Similar to Lei and Rinaldo (2015), we consider the following metric that measures the clustering performance,

$$L_1(\hat{\Theta}, \Theta) = \min_{J \in E_K} \sum_{1 \leq k \leq K} (2n_k)^{-1} \|(\hat{\Theta}J)_{G_{k^*}} - \Theta_{G_{k^*}}\|_0, \quad (4.2)$$

where $\hat{\Theta}$ can be $\hat{\Theta}^{\text{rp}}$ or $\hat{\Theta}^{\text{rs}}$, i.e., the output of the randomized spectral clustering, and E_K is the set of all $K \times K$ permutation matrices. L_1 measures the sum of the fractions of the misclustered nodes within each community. The following theorem provides an upper bound on L_1 .

Theorem 2 *Let A be an $n \times n$ adjacency matrix generated from a stochastic block model (Θ, B) , and assume that the population adjacency matrix $P = \Theta B \Theta^\top$ is of rank K , with its smallest absolute nonzero eigenvalue at least γ_n . Let $\hat{\Theta}^{\text{rp}}$ be the output of Algorithm 2 with the target rank being K , $K + r \leq n$, and the test matrix Ω has i.i.d. standard gaussian entries. Suppose (A1) holds, and there exists an absolute constant $c_2 > 0$ such that, if*

$$\frac{Kn\alpha_n}{\gamma_n^2} \leq c_2, \quad (\text{A2})$$

then with probability larger than $1 - n^{-s}$ for any $s > 0$, there exist subsets $S_k \in G_k$ for

$k = 1, \dots, K$ such that

$$L_1(\hat{\Theta}^{\text{rp}}, \Theta) \leq \sum_{k=1}^K \frac{|S_k|}{n_k} \leq c_2^{-1} \frac{Kn\alpha_n}{\gamma_n^2} \quad (4.3)$$

And for $G = \cup_{k=1}^K (G_k \setminus S_k)$, there exists a $K \times K$ permutation matrix J such that

$$\hat{\Theta}_{G^*}^{\text{rp}} J = \Theta_{G^*}. \quad (4.4)$$

The proof of Theorem 2 is provided in the **Appendix**. Actually, the proof is almost the same with that of [Lei and Rinaldo \(2015\)](#), where they provide a general framework to bound the misclustered rate of the spectral clustering based on the concentration of A from P . (A1) is needed to use the results of Theorem 1. (A2) is a technical condition which ensures the bound in (4.3) vanishes and provides the range of parameters $(K, n, \alpha_n, \gamma_n)$ for which the result is appropriate. The constant c_2 is $1/64c_1^2$ where c_1 is the constant in (4.1) as can be tracked in the proof. In addition, S_k is actually the set of nodes in G_k that are misclustered.

Following the results in Theorem 1, the bound in (4.3) is identical to that of the non-randomized spectral clustering without paying any price. The bound in (4.3) is not explicit as γ_n is related to n . To illustrate, we now consider a special case. Suppose the SBM parameterized by (Θ, B) is generated with balanced communities size n/K , and

$$P = \Theta B \Theta^\top = \Theta(\alpha_n \lambda I_K + \alpha_n(1 - \lambda) 1_K 1_K^\top) \Theta^\top, \quad (4.5)$$

where 1_K represents a K dimensional vector of 1's and λ is a constant. For matrix of form $\Theta B \Theta^\top = \Theta((g - h)I_K + h 1_K 1_K^\top) \Theta^\top$, where $g > h > 0$, the largest and smallest eigenvalues are $\frac{n}{K}(g - h) + nh$ and $\frac{n}{K}(g - h)$, respectively ([Rohe et al., 2011](#)). Hence for the case in (4.5), $\gamma_n = n\alpha_n\lambda/K$, and then the bound in (4.3) reduces to

$$\sum_{k=1}^K \frac{|S_k|}{n_k} = O(K^3/n\alpha_n).$$

Let us discuss some specific parameter settings now. When $\alpha_n = c_0 \log n/n$ and $K =$

$o((\log n)^{1/3})$, then $O(K^3/n\alpha_n)$ is $o(1)$, and note that in such parameter set-up, (A2) is satisfied automatically. On the other hand, for fixed K , $n\alpha_n$ needs to be of order $\omega(1)$ to ensure a vanishing error bound. In such case, the bound $O(1/n\alpha_n)$ is optimal in the sense that there is no estimator which is weakly consistent when $n\alpha_n = O(1)$ (see (Ahn et al., 2018) for example).

Remark 2 *In the proof of Theorem 2, we made an assumption that the k -means algorithm finds the optimal solution as in Rohe et al. (2011). Alternatively, one can use more delicate $(1 + \varepsilon)$ -approximate k -means (Kumar et al., 2004; Matoušek, 2000) as in Lei and Rinaldo (2015) to bridge the gap, where one can find a good approximate solution within a constant fraction of the optimal value.*

In the sequel, we discuss how we can utilize the estimated membership matrix $\hat{\Theta}^{\text{rp}}$ and \tilde{A}^{rp} (or A) to estimate the link probability matrix B . Without loss of generality, we assume that the permutation matrix J in (4.4) is $I_{K \times K}$. Assume we are given the true Θ , then the following $\hat{B}^{\text{rp}} = (\hat{B}_{ql}^{\text{rp}})_{1 \leq q, l \leq K}$ is the moment estimator or the maximum likelihood estimator for B ,

$$\hat{B}_{ql}^{\text{rp}} := \frac{\sum_{1 \leq i, j \leq n} A_{ij} \Theta_{iq} \Theta_{jl}}{\sum_{1 \leq i, j \leq n} \Theta_{iq} \Theta_{jl}}, \quad 1 \leq q, l \leq K. \quad (4.6)$$

However, since Θ is not known, we can naturally use $\hat{\Theta}^{\text{rp}}$ instead to obtain a plug-in estimator $\hat{\hat{B}}^{\text{rp}} = (\hat{\hat{B}}_{ql}^{\text{rp}})_{1 \leq q, l \leq K}$ for B ,

$$\hat{\hat{B}}_{ql}^{\text{rp}} := \frac{\sum_{1 \leq i, j \leq n} A_{ij} \hat{\Theta}_{iq}^{\text{rp}} \hat{\Theta}_{jl}^{\text{rp}}}{\sum_{1 \leq i, j \leq n} \hat{\Theta}_{iq}^{\text{rp}} \hat{\Theta}_{jl}^{\text{rp}}}, \quad 1 \leq q, l \leq K. \quad (4.7)$$

Moreover, since \tilde{A}^{rp} is a good approximation of A , we can replace A with \tilde{A}^{rp} to obtain another plug-in estimator $\tilde{\hat{B}}^{\text{rp}} = (\tilde{\hat{B}}_{ql}^{\text{rp}})_{1 \leq q, l \leq K}$ for B ,

$$\tilde{\hat{B}}_{ql}^{\text{rp}} := \frac{\sum_{1 \leq i, j \leq n} \tilde{A}_{ij}^{\text{rp}} \hat{\Theta}_{iq}^{\text{rp}} \hat{\Theta}_{jl}^{\text{rp}}}{\sum_{1 \leq i, j \leq n} \hat{\Theta}_{iq}^{\text{rp}} \hat{\Theta}_{jl}^{\text{rp}}}, \quad 1 \leq q, l \leq K. \quad (4.8)$$

The following theorem provides a theoretical bound for the estimator $\tilde{\hat{B}}^{\text{rp}}$.

Theorem 3 *Let A be an $n \times n$ adjacency matrix generated from a stochastic block model (Θ, B) , assume that the population adjacency matrix $P = \Theta B \Theta^\top$ is of rank K , with its smallest absolute nonzero eigenvalue at least γ_n and largest eigenvalue at most δ_n , and assume the SBM has balanced community size n/K . Let $\hat{\Theta}^{\text{rp}}$ be the output of Algorithm 2 with the target rank being K , $K+r \leq n$, and the test matrix Ω has i.i.d. standard gaussian entries. Suppose (A1) and (A2) hold, then with probability larger than $1 - K^2 n^{-s}$, for any $s > 0$,*

$$\|\tilde{B}^{\text{rp}} - B\|_\infty \leq \left(\frac{2c_1 \sqrt{K+r} K \sqrt{n\alpha_n}}{n} + \frac{\sqrt{K} K \delta_n}{n} \right) \left(1 + \left(1 - c_2^{-1} \frac{Kn\alpha_n}{\gamma_n^2}\right)^{-1} + 2 \left(1 - c_2^{-1} \frac{Kn\alpha_n}{\gamma_n^2}\right)^{-2} \right), \quad (4.9)$$

where c_1 and c_2 are the same as those arising in (4.1) and (4.3), respectively.

The proof of Theorem 3 can be found in the **Appendix**. Let us illustrate the bound in (4.9) more explicitly. Again, we consider the specific case in (4.5), where the SBM has balanced communities size n/K , and the within and between community probabilities are α_n and $\alpha_n(1-\lambda)$, respectively. In such cases, the minimum and maximum eigenvalues of P are $\gamma_n = n\alpha_n\lambda/K$ and $\delta_n = n\alpha_n\lambda/K + \alpha_n(1-\lambda)n$, respectively. Suppose further that $\alpha_n = c_0 \log n/n$, and then the bound in (4.9) reduces to

$$\|\tilde{B}^{\text{rp}} - B\|_\infty = O\left(\left\{ \frac{K^{3/2} \sqrt{\log n}}{n} + \left[\frac{K^{3/2}}{n} (\log n/K + \log n) \right] \right\} \left\{ 1 + \left(1 - K^3/\log n\right)^{-1} + \left(1 - K^3/\log n\right)^{-2} \right\} \right). \quad (4.10)$$

It is easy to see that $K^{3/2} \sqrt{\log n}/n = o(1)$, $K^{3/2} \log n/n = o(1)$, and $K^3/\log n = o(1)$ suffice to make sure that the RHS of (4.10) vanishes when n goes to infinity. And it turns out that $K = o((\log n)^{1/3})$ suffices.

Remark 3 *The above results hold similarly for \hat{B}^{rp} (see (4.7)); in other words, $K = o((\log n)^{1/3})$ suffices to ensure a vanishing bound of $\|\hat{B}^{\text{rp}} - B\|_\infty$, although the term $\sqrt{K+r}$ in (4.9) should be replaced with \sqrt{n} . Or one can use the best rank K approximation of A in (4.7) to obtain an identical bound as in (4.9).*

4.2 Random sampling

Similar to the random projection-based spectral clustering, we will derive theoretical results on the random sampling method from three aspects—namely, the derivation of \tilde{A}^{rs} from P , the misclustering error, and the derivation of \tilde{B}^{rs} from the link probability matrix B , where \tilde{B}^{rs} is an analog of \tilde{B}^{rp} in (4.8). The next theorem provides an upper spectral-norm bound for the derivation of \tilde{A}^{rs} from P .

Theorem 4 *Let A be an $n \times n$ adjacency matrix generated from a stochastic block model (Θ, B) . Assume that the $P = \Theta B \Theta^\top$ is of rank K . Let \tilde{A}^{rs} be the intermediate output in Algorithm 3 with the target rank being K , i.e., the best rank- K approximation of the sampled A with the sampling probability being p . Suppose assumption (A1) holds, then for any $\nu > 0$ and $0 < p \leq 1$, there exist constants $c_3 > 0$ and $c_4 > 0$ such that*

$$\|\tilde{A}^{\text{rs}} - P\|_2 \leq c_3 \max\left\{\sqrt{\frac{n\alpha_n}{p}}, \frac{\sqrt{\log n}}{p}, \sqrt{\frac{n\alpha_n^2}{p}} \left(1 + p^{1/4} \cdot \max\left(1, \sqrt{\frac{1}{p} - 1}\right)\right)\right\}, \quad (4.11)$$

with probability larger than $1 - 2n^{-\nu} - \exp\left(-c_4 np \left(1 + p^{1/4} \cdot \max\left(1, \sqrt{\frac{1}{p} - 1}\right)^2\right)\right)$.

We provide the proof of Theorem 4 in the **Appendix**. It is easy to see that the three terms in the RHS of (4.11) all decrease with the sampling rate p , which coincides with our intuition. For $p > 1/2$, the RHS of (4.11) reduces to $c_3 \max\left(\sqrt{n\alpha_n/p}, \sqrt{\log n/p}\right)$, which is further reduced to $O(\sqrt{\log n/p})$ if $\alpha_n = c_0 \log n/n$. And for fixed p , the bound in (4.11) is the same with the concentration bound of the full adjacency matrix A around its population P (Lei and Rinaldo, 2015) by recalling assumption (A1). In this sense, the sampled matrix \tilde{A}^{rs} can be regarded as a network sampled from the same SBM generating A , although the elements of \tilde{A}^{rs} are not binary.

Remark 4 *Li et al. (2016) also studied the derivation of \tilde{A}^{rs} from P but in the context of network cross-validation. It turns out that $K \leq n/\log n$ is required therein to ensure that the concentration bound of \tilde{A}^{rs} meets that of the full adjacency matrix A , provided that p is fixed. Compared to their treatments, we here bound \tilde{A}^{rs} differently, and it turns out that it*

can achieve the concentration bound of the full adjacency matrix A when p is fixed without requiring $K \leq n/\log n$.

The following theorem justifies the clustering performance of the randomized spectral clustering via the random sampling (Algorithm 3). Specifically, we provide an upper bound for the metric L_1 (see (4.2)) which measures the sums of the fraction of misclustered node within each true cluster.

Theorem 5 *Let A be an $n \times n$ adjacency matrix generated from a stochastic block model (Θ, B) , and assume that the population adjacency matrix $P = \Theta B \Theta^\top$ is of rank K , with its smallest absolute nonzero eigenvalue at least γ_n . Let $\hat{\Theta}^{\text{rs}}$ be the output of Algorithm 3 with the target rank being K , and the sampling probability being p . Suppose (A1) holds, and there exists an absolute constant $c_5 > 0$ such that, if*

$$K \max \left\{ \sqrt{\frac{n\alpha_n}{p}}, \frac{\sqrt{\log n}}{p}, \sqrt{\frac{n\alpha_n^2}{p}} \left(1 + p^{1/4} \cdot \max(1, \sqrt{\frac{1}{p} - 1})\right) \right\}^2 / \gamma_n^2 \leq c_5, \quad (\text{A3})$$

then with probability larger than $1 - 2n^{-\nu} - \exp\left(-c_4 np \left(1 + p^{1/4} \cdot \max(1, \sqrt{\frac{1}{p} - 1})^2\right)\right)$ for any $\nu > 0$ and $0 < p \leq 1$, there exist subsets $S_k \in G_k$ for $k = 1, \dots, K$ such that

$$L_1(\hat{\Theta}^{\text{rs}}, \Theta) \leq \sum_{k=1}^K \frac{|S_k|}{n_k} \leq (c_5 \gamma_n^2)^{-1} K \max \left\{ \sqrt{\frac{n\alpha_n}{p}}, \frac{\sqrt{\log n}}{p}, \sqrt{\frac{n\alpha_n^2}{p}} \left(1 + p^{1/4} \cdot \max(1, \sqrt{\frac{1}{p} - 1})\right) \right\}^2 \quad (4.12)$$

And for $G = \cup_{k=1}^K (G_k \setminus S_k)$, there exists a $K \times K$ permutation matrix J such that

$$\hat{\Theta}_{G^*}^{\text{rs}} J = \Theta_{G^*}. \quad (4.13)$$

The proof is similar to that of Theorem 2, hence we omit it. Indeed, the following relationship between L_1 and $\|\tilde{A}^{\text{rs}} - P\|_2$ holds,

$$L_1(\hat{\Theta}^{\text{rs}}, \Theta) \leq \frac{64K}{\gamma_n^2} \|\tilde{A}^{\text{rs}} - P\|_2^2.$$

Consider the special case of SBM in (4.5), and let p be fixed; then similar to the random

projection scheme, the bound in (4.12) reduces to $\sum_{k=1}^K \frac{|S_k|}{n_k} = O(K^3/n\alpha_n)$, which is $o(1)$ under the parameter set-up that $\alpha_n = c_0 \log n/n$ and $K = o((\log n)^{1/3})$. In addition, similar to the random projection scheme, the bound $O(K^3/n\alpha_n)$ is optimal in the sense that there is no estimator which is weakly consistent when $n\alpha_n = O(1)$ (see Ahn et al. (2018) for example).

Next, we discuss the estimation of the link probability matrix B using the estimated membership matrix $\hat{\Theta}^{\text{rs}}$ and the randomized matrix \tilde{A}^{rs} . To that end, similar to the random projection setting, we define the following plug-in estimator $\tilde{B}^{\text{rs}} = (\tilde{B}_{ql}^{\text{rs}})_{1 \leq q, l \leq K}$ for B ,

$$\tilde{B}_{ql}^{\text{rs}} := \frac{\sum_{1 \leq i, j \leq n} \tilde{A}_{ij}^{\text{rs}} \hat{\Theta}_{iq}^{\text{rs}} \hat{\Theta}_{jl}^{\text{rs}}}{\sum_{1 \leq i, j \leq n} \hat{\Theta}_{iq}^{\text{rs}} \hat{\Theta}_{jl}^{\text{rs}}}, \quad 1 \leq q, l \leq K.$$

The following theorem provides an upper bound for the derivation of $\tilde{B}^{\text{rs}} = (\tilde{B}_{ql}^{\text{rs}})_{1 \leq q, l \leq K}$ from B .

Theorem 6 *Let A be an $n \times n$ adjacency matrix generated from a stochastic block model (Θ, B) ; assume that the population adjacency matrix $P = \Theta B \Theta^\top$ is of rank K , with its smallest absolute nonzero eigenvalue at least γ_n and largest eigenvalue at most δ_n ; and assume the SBM has balanced community size n/K . Let $\hat{\Theta}^{\text{rs}}$ be the output of Algorithm 3 with the target rank being K , and the sampling probability being p . Suppose (A1) and (A3) hold, then with probability larger than $1 - 2Kn^{-\nu} - K \exp(-c_4 np(1 + p^{1/4} \cdot \max(1, \sqrt{\frac{1}{p} - 1})^2))$ for any $\nu > 0$ and $0 < p \leq 1$,*

$$\|\tilde{B}^{\text{rs}} - B\|_\infty \leq \left(\frac{2c_3 \sqrt{K + r} K \cdot \text{err}}{n} + \frac{\sqrt{K} K \delta_n}{n} \right) \left(1 + (1 - c_5^{-1} \frac{K \cdot \text{err}^2}{\gamma_n^2})^{-1} + 2(1 - c_5^{-1} \frac{K \cdot \text{err}^2}{\gamma_n^2})^{-2} \right), \quad (4.14)$$

where

$$\text{err} := \max \left\{ \sqrt{\frac{n\alpha_n}{p}}, \frac{\sqrt{\log n}}{p}, \sqrt{\frac{n\alpha_n^2}{p}} \left(1 + p^{1/4} \cdot \max(1, \sqrt{\frac{1}{p} - 1}) \right) \right\}, \quad (4.15)$$

and c_3 and c_5 are the same as those arising in (4.11) and (4.12), respectively.

We omit the proof since it is similar to that of Theorem 3. We can discuss the bound in

(4.14) in a similar way to the random projection scheme. For example, under the special case of SBM in (4.5) and assuming $\alpha_n = c_0 \log n / n$ and p is fixed, then the bound in (4.14) reduces to

$$\|\tilde{B}^{\text{rs}} - B\|_\infty = O\left(\left\{\frac{K^{3/2}\sqrt{\log n}}{n} + \left[\frac{K^{3/2}}{n}(\log n / K + \log n)\right]\right\}\{1 + (1 - K^3 / \log n)^{-1} + (1 - K^3 / \log n)^{-2}\}\right), \quad (4.16)$$

which is identical to (4.10). Thus $K = o((\log n)^{1/3})$ suffices to make sure that the RHS of (4.16) vanishes when n goes to infinity.

4.3 Discussion of the results

In the above theorems, we have analyzed the randomized spectral clustering in terms of the approximation error, the misclustering error, and the estimation error for the link probability matrix. For the approximation error, we mean the bound for $\|\tilde{A} - P\|_2$, where \tilde{A} can be \tilde{A}^{rp} or \tilde{A}^{rs} . At the first glance, one can upper bound it using the existing bound of $\|\tilde{A} - A\|_2$ (see Halko et al. (2011) for example) and $\|A - P\|_2$ (see Lei and Rinaldo (2015) for example) by noting,

$$\|\tilde{A} - P\|_2 \leq \|\tilde{A} - A\|_2 + \|A - P\|_2, \quad (4.17)$$

where the term in the RHS can be thought of as an ‘‘approximation’’ error and a statistical error, respectively. However, this kind of derivation may bring unnecessary error since one did not make use of the structure of \tilde{A} and the exact low rank nature of P when deriving the inequality in (4.17). Instead, as can be seen in the proofs, we rearrange the term $\tilde{A} - P$ according to the structure and property of \tilde{A} with respect to the two randomized schemes, respectively. And it turns out that we should use the bound of $\|\tilde{P} - P\|_2$ instead to bound $\|\tilde{A} - P\|_2$ such that the approximation error bound can be largely reduced. For the misclustering error, we mean the sum of the fraction of misclustered nodes within each true cluster up to some permutations. We make use of the Davis-Kahan theorem to analyze the eigenvector perturbation, and then the misclustering error can be bounded based on the eigen-structure of SBM (Lemma 1). This framework for bounding the misclustering

error has been widely used in [Rohe et al. \(2011\)](#); [Lei and Rinaldo \(2015\)](#); [Chin et al. \(2015\)](#); [Gao et al. \(2017\)](#), among many others. For the estimation of the link probability matrix B , we derive a simple plug-in estimator based on the estimated clusters and approximated adjacency matrix \tilde{A} or the adjacency matrix A . And we mainly use the upper bound of the eigenvalues of P , and the misclustering error bound to derive the estimation bound for B . To the best of our knowledge, this bound is rarely studied in the context of spectral clustering.

The theoretical bounds show satisfactory performance of the randomized spectral clustering. In particular, the approximation error bounds of randomized spectral clustering algorithms are the same as the best known concentration bound of $\|A - P\|_2$ ([Lei and Rinaldo, 2015](#); [Chin et al., 2015](#); [Gao et al., 2017](#)), provided that the test matrix in the random projection scheme being i.i.d. standard gaussian and the sampling rate in the random sampling scheme being fixed. Hence it seems as if the randomized adjacency matrix is sampled from a SBM. The misclustering error implies that the randomized spectral clustering are weakly consistent in the sense that the the fraction of the misclustered nodes vanishes as n goes to infinity. And the misclustering error bounds are optimal in the sense that there is no estimator which is weakly consistent when $n\alpha_n = O(1)$, and K and p are fixed, where K denotes the number of communities, α_n denotes the maximum probability of an edge, and p is the sampling rate in the random sampling scheme. As for the link probability error, we show that it vanishes under mild conditions. Note that we focus on the pure spectral clustering without refinement or regularization, which is studied mainly by [Rohe et al. \(2011\)](#) and [Lei and Rinaldo \(2015\)](#) under the SBM framework but without randomization. It turns out that the approximation error bounds and the misclustering error bounds are identical to that in [Lei and Rinaldo \(2015\)](#), provided that the test matrix in the random projection scheme being i.i.d. standard gaussian and the sampling rate in the random sampling scheme being fixed.

Some authors study the spectral clustering with regularization or refinement, see [Gao et al. \(2017\)](#); [Qin and Rohe \(2013\)](#); [Yun and Proutiere \(2014, 2016\)](#), among many others. These treatments can lead to better misclustering error bounds or help the refined spectral

clustering achieves the information-theoretic limit of the exact recovery problem in SBMs. Very recently, a few authors study the entrywise perturbation of eigenvectors for matrices whose expectations are low-rank, which leads to new and sharp theoretical guarantees, see [Abbe et al. \(2019\)](#) and [Xia and Yuan \(2019\)](#) for example. The results imply that the pure spectral clustering algorithm achieves the information-theoretic limit of exact recovery without any trimming or refining steps ([Abbe et al., 2019](#)). It would be of interest to study whether similar results hold for the randomized spectral clustering.

5 Numerical Results

In this section, we empirically compare the finite sample performance of the randomized spectral clustering, namely, the random projection and the random sampling, with the original spectral clustering. To that end, we first carry out simulations to evaluate the theoretical bounds derived in Section 4, then we conduct another series of simulations to see how the clustering performance of the randomized spectral clustering changes accordingly as the input parameters change.

To be consistent with Section 4, we use the following three metrics to evaluate the theoretical performance of each method. The first one is the spectral derivation of the “approximated” adjacency matrix \tilde{A} from the population adjacency matrix P , namely, $\|\tilde{A} - P\|_2$, where \tilde{A} can be \tilde{A}^{rs} , \tilde{A}^{rp} or A . The second metric is the sum of the fractions of misclustered nodes within each true cluster, namely,

$$\min_{J \in E_K} \sum_{1 \leq k \leq K} (2n_k)^{-1} \|(\hat{\Theta}J)_{G_{k*}} - \Theta_{G_{k*}}\|_0,$$

where $\hat{\Theta}$ can be $\hat{\Theta}^{\text{rp}}$, $\hat{\Theta}^{\text{rs}}$ or $\hat{\Theta}$. The third metric is the derivation of the estimated link probability matrix $\tilde{\tilde{B}}$ from the true link probability matrix B , namely, $\|\tilde{\tilde{B}} - B\|_\infty$ and recalling (4.10), where $\tilde{\tilde{B}}$ can be $\tilde{\tilde{B}}^{\text{rp}}$, $\tilde{\tilde{B}}^{\text{rs}}$, or the counterpart corresponding to the original spectral clustering. Throughout this section, the SBMs parameterized by (Θ, B) were

homogeneously generated in the following way,

$$P = \Theta B \Theta^\top = \Theta(\alpha_n \lambda I_K + \alpha_n(1 - \lambda) \mathbf{1}_K \mathbf{1}_K^\top) \Theta^\top,$$

where $\mathbf{1}_K$ represents a K dimensional vector of 1's and λ is a constant, and the community sizes are balanced to be n/K . To see how the above mentioned metrics change with n , K , α_n , we conduct the following four experiments.

Experiment 1. In this experiment, we aim to evaluate the effect of n on the three metrics. To that end, we let n vary while keeping the other parameters fixed as $K = 3, \alpha_n = 0.2, \alpha_n(1 - \lambda) = 0.1$. The oversampling parameter, the power parameter, and the random test matrix Ω in the random projection were set to be $r = 10, q = 2$, and with i.i.d. standard gaussian entries, respectively. The sampling rate p in the random sampling scheme was set as 0.7. Figure 1 shows the average results of 20 replications, where “non-random” refers to the original spectral clustering. Recall that the error bound for P increases with order $O(\sqrt{n})$, the error bound for Θ decreases with order $O(1/n)$, and the error bound for B vanishes as n goes to infinity. As expected, from Figure 1 we can see that the empirical results are consistent with the theoretical bound in some sense. The randomized methods perform worse than the original spectral clustering when n is small, say $n < 600$, but they become almost identical when n becomes large, say $n > 800$, which is actually the focus of this paper (see Figure 1(b) and (c)). As for the approximation error, we see that the random projection and the random sampling perform better and worse, respectively, than the original spectral clustering (see Figure 1(a)). Indeed, in Section 4, we proved $\|A^{\text{rp}} - P\|_2 \leq \|A - P\|_2$ with high probability. Thus further investigation of the spectral norm bound $\|A^{\text{rp}} - P\|_2$ is needed, while for $\|A^{\text{rs}} - P\|_2$, we think it is larger than $\|A - P\|_2$ due to the constant terms. The same explanation of the error bound for P holds for the following experiments.

Experiment 2. In this experiment, we evaluate the effect of α_n on the three metrics. We fix the sample size for the moment, and focus on the influence of the maximum link probability α . Specifically, we let α vary and the between cluster probability was set as $\alpha(1 - 0.5)$ varying with α . The sample size n was fixed at 1152. The other parameters were

the same as those in Experiment 1. Figure 2 displays the average results of 20 replications. By the theoretical results, we know that the error bound for P increases with order $O(\sqrt{\alpha})$, the error bound for Θ decreases with order $O(1/\alpha_n)$, and the error bound for B decreases ultimately after some increase at the beginning as α increases. The empirical results in Figure 2 coincide with the theoretical results in some sense. And the gap between the randomized and the original spectral clustering closes as α increases.

Experiment 3. In this experiment, we test the effect of K on the three metrics. Specifically, we let K vary, the within cluster probability $\alpha = 0.2$, and the between cluster probability $\alpha(1 - 0.5) = 0.1$, respectively. The other parameters were the same as those in Experiment 2. The average results of 20 replications are shown in Figure 3. The theoretical bounds indicate that the error bound for Θ increases with order $O(K^3)$, and the error bound for B increases with K . As expected, the empirical results support the theoretical findings (see Figure 3(b) and (c)). While for the approximation error $\|A - P\|_2$, recall that the bound in [Lei and Rinaldo \(2015\)](#) holds for any A with independent entries and $\mathbb{E}(A) = P$, and they do not make the assumption that P corresponds to a SBM. Hence the theoretical bound has nothing to do with K . Empirically, from Figure 3(a) we see that the approximation error for P decreases slightly as K increases, which shows that the K in fact has negligible effect on the approximation error, although theoretically we has not taken K into consideration.

Experiment 4. In the above three experiments, we fixed all the other parameters except the one that we pay attention to. Indeed, in view of the theoretical bounds, all the parameters can vary with n . To see the so-called high-dimensional performance of each method, in this experiment, we consider a simple setting that the within cluster and between cluster probabilities decrease with n according to $\alpha_n = 2/\sqrt{n}$ and $\alpha_n(1 - 0.5) = 1/\sqrt{n}$, respectively. In such setting, to ensure the decreasing trend of the misclustered error, K should be of smaller order than $n^{1/6}$, which is rather small for n smaller than, say, 1000. Hence we set $K = 2$ for simplicity. The other parameters were the same as those in Experiment 2. Figure 4 shows the average curves for each method in terms of three metrics. As expected, the misclustering error and the error for B both decrease as n

increases, showing the high-dimensional feature of the theoretics.

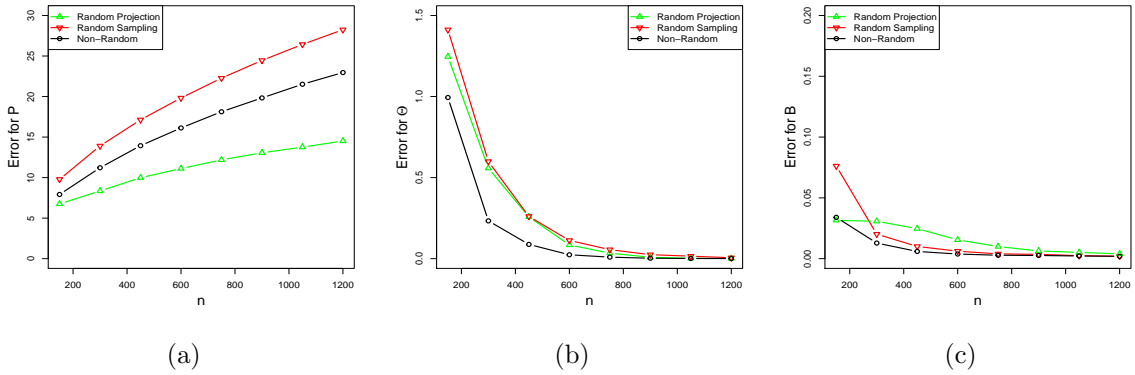


Figure 1: The average effect of n on the three metrics over 20 replications. (a), (b), (c) correspond to the approximation error for P , the misclustered error for Θ , and the estimation error for B , respectively. The other parameters $K = 3, \alpha_n = 0.2, \alpha_n(1-\lambda) = 0.1, r = 10, q = 2, p = 0.7$, and Ω had i.i.d. standard gaussian entries, respectively.

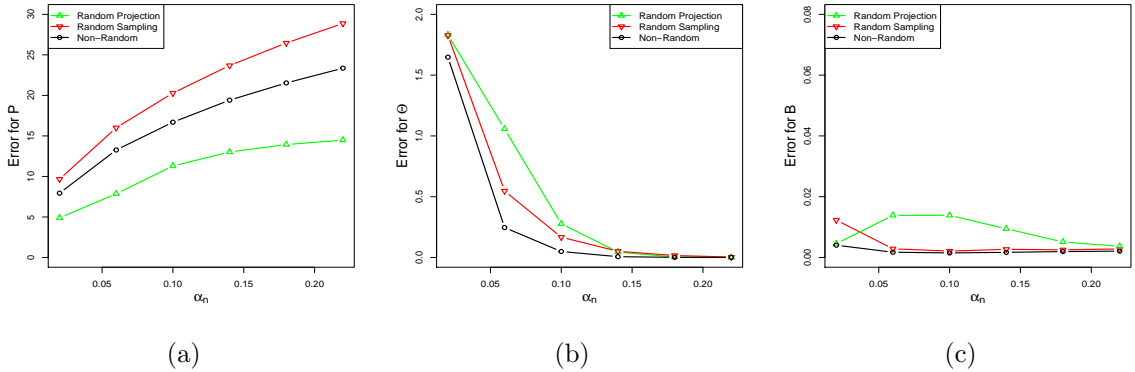


Figure 2: The average effect of α on the three metrics over 20 replications. (a), (b), (c) correspond to the approximation error for P , the misclustered error for Θ , and the estimation error for B , respectively. The other parameters $n = 1152, K = 3, \lambda = 0.5, r = 10, q = 2, p = 0.7$, and Ω had i.i.d. standard gaussian entries, respectively.

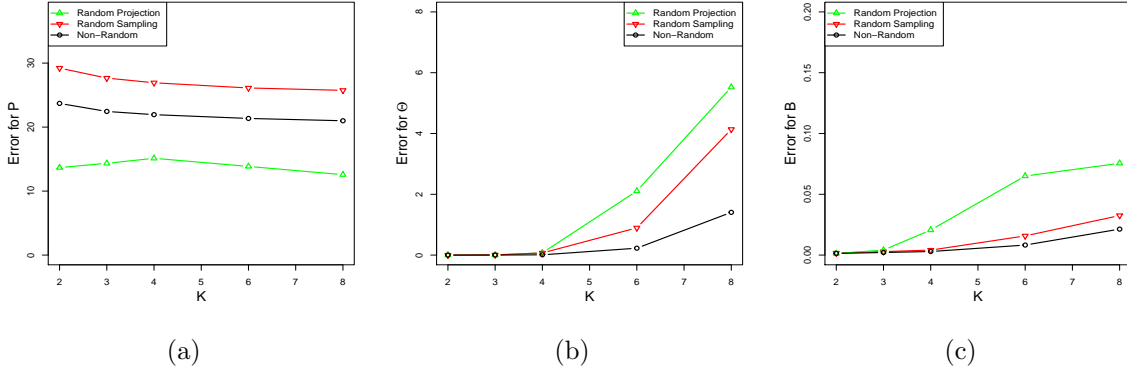


Figure 3: The average effect of K on the three metrics over 20 replications. (a), (b), (c) correspond to the approximation error for P , the misclustered error for Θ , and the estimation error for B , respectively. The other parameters $n = 1152$, $\alpha_n = 0.2$, $\alpha_n(1 - \lambda) = 0.1$, $r = 10$, $q = 2$, $p = 0.7$, and Ω had i.i.d. standard gaussian entries, respectively.

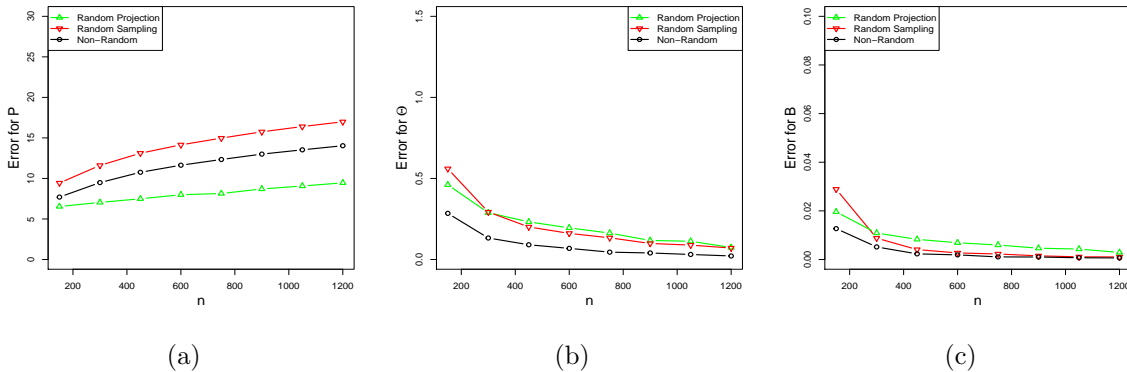
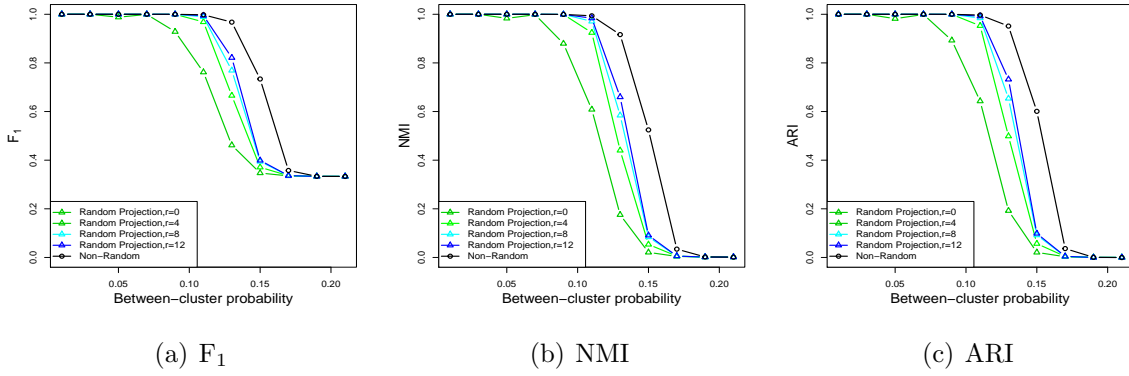


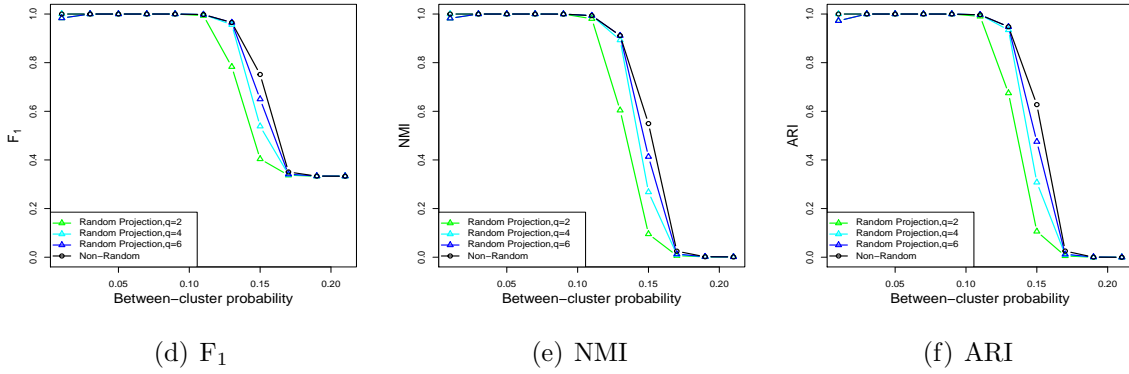
Figure 4: The average effect of n and α_n on the three metrics over 20 replications. (a), (b), (c) correspond to the approximation error for P , the misclustered error for Θ , and the estimation error for B , respectively. The within cluster probability $\alpha_n = 2/\sqrt{n}$ and the between cluster probability $\alpha_n(1 - 0.5) = 1/\sqrt{n}$. The other parameters $K = 2$, $r = 10$, $q = 2$, $p = 0.7$, and Ω had i.i.d. standard gaussian entries, respectively.

Till now, we have tested the efficacy of the theoretical bounds. Note that in the above experiments, many parameters were fixed, including the oversampling parameter r , the power parameter q , the distribution of the random test matrix within the random projection scheme, and the sampling rate p within the random sampling scheme. To see how these parameters affect the performance of each method, we here conduct another series of experiments. Specifically, to remove the computational cost of finding the best permutation matrix over the permutation matrix set, we use F_1 score (F_1), Normalized Mutual Information (NMI), and Adjusted Rand Index (ARI) (Manning et al., 2010) to justify the clustering performance of each method. These indexes measure the similarity of two clusters, and here we refer to the estimated and true clusters, from different perspectives. The larger these indexes, the better the clustering algorithm performs. The parameters were basically set as $n = 1152$, $K = 3$, and the within cluster probability $\alpha = 0.2$. To see the effect of other parameters, we varied the oversampling parameter $r \in \{0, 4, 8, 12\}$, the power parameter $q \in \{2, 4, 6\}$, the sampling rate $p \in \{0.6, 0.7, 0.8, 0.9\}$, and the distribution of test matrix Ω was generated as i.i.d. gaussian (standard), uniform (from -1 to 1), and rademacher (take values +1 and -1 with equal probability). And for each setting, we let the between cluster probability vary. Figure 5 and 6 show the average results of the random projection scheme and the random sampling scheme, respectively. As expected, larger r , q and p lead to better clustering performance but at the cost of computational efficiency. One should choose these parameters according to the problem at hand. In addition, among the distribution of Ω we tested, it has little effect on the resulting clustering performance of random projection.

(a₁) Effect of the oversampling parameter r



(a₂) Effect of the power parameter q



(a₃) Effect of the test matrix Ω

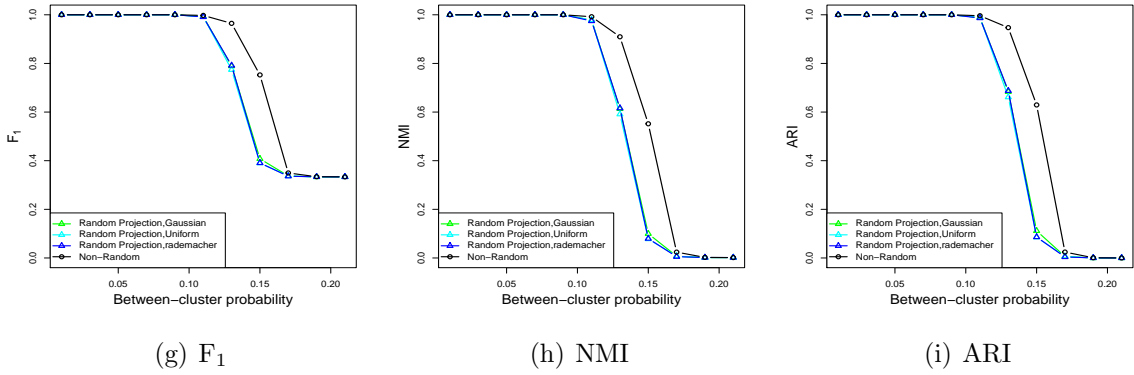


Figure 5: Effects of the parameters r, q, Ω in the random projection scheme. Each row corresponds to the effect of one parameter with the others fixed. Each column corresponds to a measure for the clustering performance. The other parameters are fixed at $n = 1152$, $K = 3$, and the within cluster probability $\alpha = 0.2$.

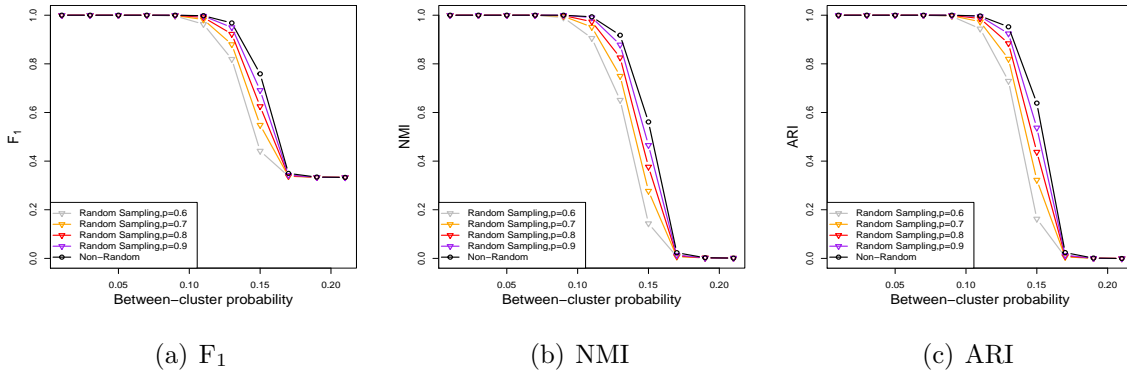


Figure 6: Effect of the parameters p within the random sampling scheme. Each column corresponds to a measure for the clustering performance. The other parameters are fixed at $n = 1152$, $K = 3$, and the within cluster probability $\alpha = 0.2$.

6 Real data examples

In this section, we test the effectiveness of randomized spectral clustering on four network datasets, including the European email network, the political blog network, the statistician coauthor network, and the statistician citation network, where the first two datasets have ground truth community assignments and the last two have no ground truth community assignment. We will introduce each dataset in detail in the sequel. For the datasets with ground truth labels, we computed F_1 , NMI, and ARI (Manning et al., 2010) between the estimated clusters and the true clusters for each of the three methods, namely, the random projection, the random sampling, and the original spectral clustering, respectively. While for the datasets without ground truth labels, we computed F_1 , NMI, and ARI between the clusters estimated by the randomized spectral clustering and the clusters estimated by the original spectral clustering. Our aim is to show that randomized algorithms perform comparably to the original spectral clustering. Hence for the datasets without ground truth labels, the smaller gap of F_1 , NMI, and ARI between randomized and original spectral clustering indicate the better match between these methods. While for the datasets with ground truth labels, larger F_1 , NMI, and ARI indicates the better match. For the random projection scheme, the oversampling parameter $r = 10$, the power parameter $q = 2$, and the random test matrix had i.i.d. gaussian entries. And for the random sampling scheme,

we tested two cases, namely, $p = 0.7, 0.8$. Table 2 summarizes the average performance of these methods over 50 replications with the standard deviations in the parentheses.

European email network. The network was generated using the email data from a large European research institution (Leskovec et al., 2007; Yin et al., 2017). Each individual belongs to exactly one of 42 departments at the research institute, which are treated as the ground truth community assignments. An edge exists if one of individuals representing the edge endpoints sent at least one mail to the other. We consider the largest connected component of the “core” of the email network (Yin et al., 2017), which consists of 986 nodes (see Figure 7(a)). Table 2 shows that the clustering performance of randomized spectral clustering was comparable to that of the original spectral clustering. Note that the randomized spectral clustering may have slightly larger F_1 , NMI, or ARI than those of the original spectral clustering due to the randomness in all these algorithms.

Political blog network. The network was generated using the well-known political blog datasets collected during the 2004 US presidential election (Adamic and Glance, 2005). All edges, which were originally directed, were made undirected by assigning an edge between two nodes if there is an edge between them in either direction. According to the political leanings of the blogs, the nodes are split into two groups, conservative and liberal, which we treated as the ground truth assignments. We consider the largest connected component of the network which includes 1222 nodes (see Figure 7(b)). From Table 2 we see that all the methods perform very similarly to each other in terms of F_1 , NMI, and ARI, and the results are rather stable, which shows the effectiveness of randomized methods.

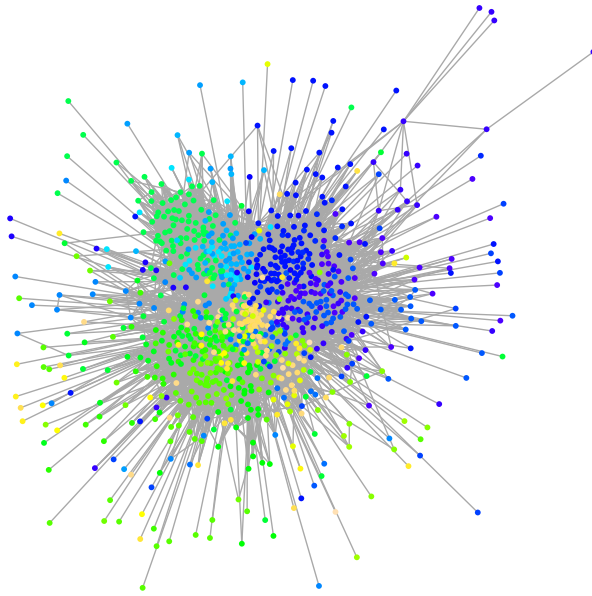
Statisticians coauthor network. The dataset was collected by Ji and Jin (2016) on the basis of all published papers from 2003 to the first half of 2012 in four of the top statistical journals: Annals of Statistics, Journal of Royal Statistical Society (Series B), Journal of American Statistical Association and Biometrika, which results in 3607 authors and 3248 papers in total. We here study a coauthor network based on this dataset where nodes represent authors and there is an undirected edge between two authors if and only if they have coauthored one or more papers. We consider the largest connected components of this network which contains 2263 nodes. Following Ji and Jin (2016), we set $K = 3$.

Since this network has no ground truth assignments, we compare the resulting clusters of the randomized methods to that of the original spectral clustering in terms of F_1 , NMI, and ARI. Table 2 shows that those three metrics are large, especially for the F_1 , which indicates the comparability of the randomized and original spectral clustering. It turns out that the clustering results are very similar for the three methods. All three methods yield clusters that consist of statisticians where a large majority of them are engaged in bayesian statistics, biostatistics, and high-dimensional statistics, respectively. The results are similar to those in Ji and Jin (2016).

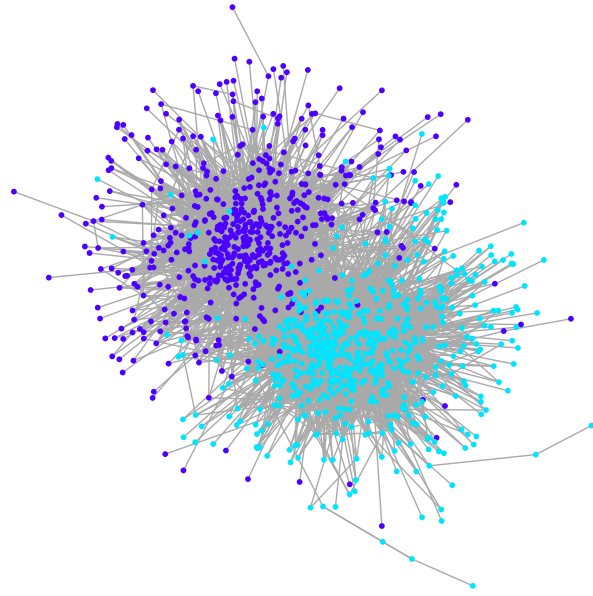
Statisticians citation network. The network was also generated based on the above mentioned dataset (Ji and Jin, 2016). We here study a citation network where there is an undirected edge between two authors if and only if either of the authors has cited one or more papers by the other author. And we consider the largest connected components of this network that includes 2654 nodes. We set $K = 3$ as in Ji and Jin (2016). Table 2 shows that the community detection results are very similar for the three methods, suggested by the large F_1 , NMI, and ARI. As a result, all three methods find clusters that consist of statisticians where a large majority of them are engaged respectively in large-scale multiple testing, high-dimensional statistics, and spatial and semiparametric/nonparametric statistics, showing the efficacy of the randomized spectral clustering.

Table 2: The clustering performance of each method on four real network datasets. For the European email network and political blog network, the performance is evaluated based on a known ground truth. For the statisticians coauthor citation networks, the performance is evaluated based on the original spectral clustering.

Method	F ₁	NMI	ARI
(a) European email network			
Random Projection	0.161(0.008)	0.563(0.006)	0.096(0.009)
Random Sampling ($p = 0.7$)	0.148(0.008)	0.539(0.008)	0.080(0.010)
Random Sampling ($p = 0.8$)	0.151(0.006)	0.552(0.008)	0.084(0.007)
Non-Random	0.154(0.006)	0.569(0.005)	0.088(0.007)
(b) Political blog network			
Random Projection	0.641(0.003)	0.178(0.003)	0.079(0.004)
Random Sampling ($p = 0.7$)	0.642(0.000)	0.178(0.006)	0.078(0.005)
Random Sampling ($p = 0.8$)	0.642(0.003)	0.177(0.006)	0.078(0.006)
Non-Random	0.641(0.004)	0.178(0.004)	0.079(0.006)
(c) Statisticians coauthor network (No labels)			
Random Projection (relative)	0.983(0.013)	0.682(0.201)	0.746(0.253)
Random Sampling (relative) ($p = 0.7$)	0.970(0.011)	0.490(0.154)	0.580(0.187)
Random Sampling (relative) ($p = 0.8$)	0.973(0.013)	0.544(0.169)	0.630(0.217)
(d) Statisticians citation network (No labels)			
Random Projection (relative)	0.986(0.030)	0.869(0.197)	0.909(0.182)
Random Sampling (relative) ($p = 0.7$)	0.977(0.025)	0.730(0.160)	0.834(0.159)
Random Sampling (relative) ($p = 0.8$)	0.982(0.022)	0.786(0.157)	0.871(0.148)



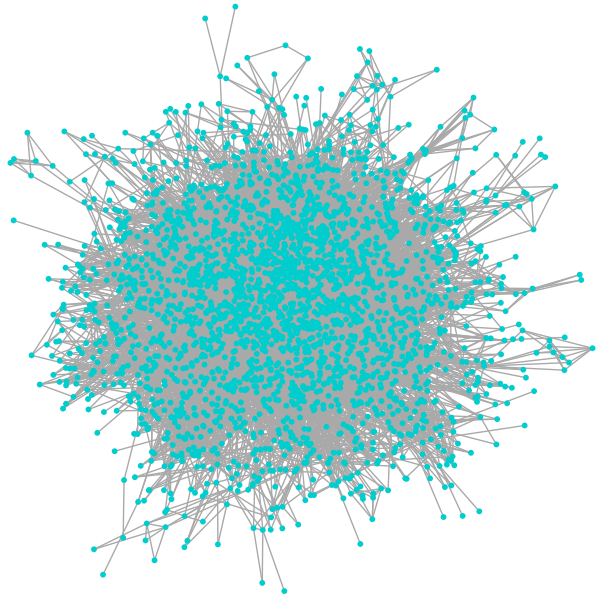
(a) European email network



(b) Political blog network



(c) Statisticians coauthor network



(d) Statisticians citation network

Figure 7: The four networks used in the real data analysis. Each network corresponds to the largest connected components of the original networks. (a) The European email network with $n = 986$ and $K = 42$. (b) The political blog network with $n = 1222$ and $K = 2$. (c) The statisticians coauthor network with $n = 2263$. (d) The statisticians citation network with $n = 2654$.

7 Conclusion

In this paper, we used randomized sketching techniques to accelerate the original spectral clustering when facing large-scale networks and studied how well the resulting algorithms perform under the stochastic block models. We studied two randomized spectral clustering algorithms. The first one is random projection-based, which reduces the computational cost by projecting the columns and rows of the adjacency matrix to a lower-dimensional space. The second one is random sampling-based, which samples the node pairs to obtain a sparsified adjacency matrix, and thus the computational cost is reduced. In the framework of SBMs, we studied these two randomized spectral clustering algorithms in terms of the approximation error that measures the derivation of the randomized adjacency matrix \tilde{A} from the population matrix P , the misclustering error that measures the fraction of the number of misclustered nodes over the total number of nodes, and the error for the link probability matrix B . It turns out that under mild conditions, the approximation error with respect to \tilde{A} is the same as that with respect to the original adjacency matrix A , which shows that the randomized matrix behaves as if it was sampled from the SBM. And the bounds are to the best of our knowledge the same as the best concentration bound of $\|A - P\|_2$ (Chin et al., 2015; Gao et al., 2017; Lei and Rinaldo, 2015). Similarly, the misclustering error rates are the same for the randomized and non-randomized spectral clustering algorithms under mild conditions. And they are optimal when the community number K is fixed. In addition, the error for the link probability matrix vanishes as the number of nodes grows, which has not been mentioned in most of the literature on the spectral clustering. Finally, the experimental results support our theoretical results.

There are many ways that the content in this paper can be extended. First, we studied the weak consistency of the pure spectral clustering without any regularization or refinement, where the weak consistency refers to the notion that the fraction of misclustered nodes vanishes as the total number of nodes tends to infinity, and we mainly used the Davis-Kahan theorem to study the eigenvector perturbation. As mentioned in Section 4, there exist several works on trimming or refining the original spectral clustering to help the refined spectral clustering achieve the information-theoretic limit of the exact recovery in

SBMs; see [Gao et al. \(2017\)](#); [Yun and Proutiere \(2016\)](#), among others. On the other hand, a few works study the entrywise perturbation of eigenvectors very recently; see [Abbe et al. \(2019\)](#) for example, which leads to new theoretical tools and results on pure spectral clustering. It turns out that pure spectral clustering can achieve the information-theoretic limit of exact recovery without any trimming steps. It would be interesting to study whether one can take advantage of these theoretical developments to improve the bounds of randomized spectral clustering. Second, we studied two particular sketching approaches. It is natural to ask whether one can improve the performance of spectral clustering statistically using other sketching methods. Finally, we mainly focused on the adjacency matrix sampled from a stochastic block model. It would be important and interesting to generalize the results to the laplacian matrix and other network generating models, say—the degree corrected stochastic block model, the latent space model, and the graphon models, among others.

Appendix

This section includes the proofs for Theorem 1-Theorem 4, respectively.

Proof of Theorem 1

We use the concentration bound of the non-randomized A around P (Lei and Rinaldo (2015); Chin et al. (2015); Gao et al. (2017)) and the argument about the low-rank randomized approximation in Halko et al. (2011) to bound the derivation of \tilde{A}^{rp} from P .

We begin by noting that

$$\begin{aligned}
 \|\tilde{A}^{\text{rp}} - P\|_2 &= \|QQ^\top AQQ^\top - P\|_2 = \|QQ^\top(A - P)QQ^\top + QQ^\top PQQ^\top - P\|_2 \\
 &\leq \|QQ^\top(A - P)QQ^\top\|_2 + \|QQ^\top PQQ^\top - P\|_2 \\
 &\leq \|A - P\|_2 + \|QQ^\top PQQ^\top - P\|_2 \\
 &=: \mathcal{I}_1 + \mathcal{I}_2
 \end{aligned} \tag{A.1}$$

where the last inequality follows from the fact that $\|AB\|_2 \leq \|A\|_2\|B\|_2$ for any matrices A and B , and $\|QQ^\top\|_2 \leq 1$ which is implied by $(QQ^\top)^2 = QQ^\top$. Next we bound $\mathcal{I}_1 = \|A - P\|_2$ and $\mathcal{I}_2 = \|QQ^\top PQQ^\top - P\|_2$, respectively.

For \mathcal{I}_1 , Lei and Rinaldo (2015) use the delicate combinatorial argument to provide a sharp bound. That is, assume

$$\max_{kl} B_{kl} \leq \alpha_n \text{ for some } \alpha_n \geq c_0 \log n/n,$$

then for any $s > 0$, there exists a constant $c_1 = c_1(s, c_0)$ such that

$$\|A - P\|_2 \leq c_1 \sqrt{n\alpha_n}. \tag{A.2}$$

with probability at least $1 - n^{-s}$.

For \mathcal{I}_2 , we first note that

$$\begin{aligned}
\|P - QQ^\top PQQ^\top\|_2 &= \|P - QQ^\top P + QQ^\top P - QQ^\top PQQ^\top\|_2 \\
&\leq \|P - QQ^\top P\|_2 + \|QQ^\top(P - PQQ^\top)\|_2 \\
&\leq 2\|P - QQ^\top P\|_2.
\end{aligned} \tag{A.3}$$

Then, we use the argument in Theorem 9.1 of [Halko et al. \(2011\)](#) to bound $\|P - QQ^\top P\|_2$. To that end, we first deal with the case that $Y = P\Omega$, where recall that Ω is the $n \times (K + r)$ random test matrix and Y is the sketch matrix, then we move on to the power iteration scheme. For illustration, we now provide some notation. Partition the eigenvalue decomposition of P as follows,

$$P = U \begin{bmatrix} \Sigma_1 & \\ & 0 \end{bmatrix} \begin{bmatrix} U_1^\top \\ U_2^\top \end{bmatrix}, \tag{A.4}$$

where $U \in \mathbb{R}^{n \times n}$, $U_1 \in \mathbb{R}^{n \times K}$, $U_2 \in \mathbb{R}^{n \times (n-K)}$, and $\Sigma_1 \in \mathbb{R}^{K \times K}$. And denote $\Omega_1 = U_1^\top \Omega$ and $\Omega_2 = U_2^\top \Omega$. With this notation, the sketch matrix Y can be written as

$$Y = P\Omega = U \begin{bmatrix} \Sigma_1 \Omega_1 \\ 0 \end{bmatrix}. \tag{A.5}$$

Further denote

$$\tilde{P} = U^\top P = \begin{bmatrix} \Sigma_1 U_1^\top \\ 0 \end{bmatrix}, \tilde{Y} = \tilde{P}\Omega = \begin{bmatrix} \Sigma_1 \Omega_1 \\ 0 \end{bmatrix}, \text{ and } \mathcal{P}_Y = QQ^\top \tag{A.6}$$

Then we have the following observations,

$$\|P - QQ^\top P\|_2 = \|(I - \mathcal{P}_Y)P\|_2 = \|U^\top(I - \mathcal{P}_Y)U\tilde{P}\|_2 = \|(I - \mathcal{P}_{U^\top Y})\tilde{P}\|_2 = \|(I - \mathcal{P}_{\tilde{Y}})\tilde{P}\|_2, \tag{A.7}$$

where the first equality follows from the *unitary invariance* of the spectral norm, that is,

$\|UAU^\top\|_2 = \|A\|_2$ for any *unitary* (square orthonormal) matrix U , i.e., $UU^\top = U^\top U = I$, and the second equality is due to the following fact (Proposition 8.4 in [Halko et al. \(2011\)](#)) that for any unitary matrix U ,

$$U^\top \mathcal{P}_M U = \mathcal{P}_{U^\top M}. \quad (\text{A.8})$$

As a result, the RHS of (A.7) is 0 because

$$\text{range}(\tilde{P}) = \text{range} \begin{bmatrix} \Sigma_1 U_1^\top \\ 0 \end{bmatrix} = \text{range} \begin{bmatrix} \Sigma_1 \Omega_1 \\ 0 \end{bmatrix} = \text{range}(\tilde{Y}), \quad (\text{A.9})$$

where we used the fact that U_1 is of full column rank and Ω_1 is of full row rank with probability 1 because of the assumption that the test matrix Ω has i.i.d. standard gaussian entries. Till now, we have verified $\mathcal{I}_2 = 0$ for the case that $Y = P\Omega$. When $Y = (P^\top P)^q P\Omega$, by the Theorem 9.2 of [Halko et al. \(2011\)](#),

$$\|(I - \mathcal{P}_Y)P\|_2 \leq \|(I - \mathcal{P}_Y)(P^\top P)^q P\|_2^{1/(2q+1)} = 0, \quad (\text{A.10})$$

where the last equality is implied by the case with $Y = P\Omega$ and the fact that rank of $(P^\top P)^q P$ is not larger than K . Hence, $\mathcal{I}_2 = 0$.

Consequently, we arrive at the conclusion of Theorem 1. ■

Proof of Theorem 2

We make use of the framework in [Lei and Rinaldo \(2015\)](#) to bound the misclustered rate. To fix ideas, we recall some notation now. U and \tilde{U}^{rp} denote the K leading eigenvectors of $P = \Theta B \Theta^\top$ and \tilde{A}^{rp} (the output of Algorithm 2), respectively. $\hat{\tilde{U}}^{\text{rp}} := \hat{\Theta}^{\text{rp}} \hat{X}^{\text{rp}}$ denotes output of the randomized spectral clustering (Algorithm 2). Recall that the heuristic of spectral clustering under the SBM lies in that two nodes are in the same community if and only if their corresponding rows of U are the same ([Lei and Rinaldo \(2015\)](#); [Rohe et al. \(2011\)](#)). Based on these facts, in what follows, we first bound the derivation of $\hat{\tilde{U}}^{\text{rp}}$ from U . Then, for those nodes within each true cluster that correspond to a large derivation of $\hat{\tilde{U}}^{\text{rp}}$

from U , we bound their size. At last, we show that for the remaining nodes, the estimated and true clusters coincide.

First, we bound the derivation of \tilde{U}^{rp} from U . Davis-Kahan $\sin\Theta$ theorem (Theorem VII.3.1 of [Bhatia \(1997\)](#)) provides a useful tool for bounding the perturbation of eigenvectors from the perturbation of matrices. Specifically, by Proposition 2.2 of [Vu and Lei \(2013\)](#), there exists a $K \times K$ orthogonal matrix O such that,

$$\|\tilde{U}^{\text{rp}} - UO\|_{\text{F}} \leq \frac{2\sqrt{2K}}{\gamma_n} \|\tilde{A}^{\text{rp}} - P\|_2. \quad (\text{A.11})$$

Now we proceed to derive the Frobenius error of \hat{U}^{rp} . Note that

$$\begin{aligned} \|\hat{U}^{\text{rp}} - UO\|_{\text{F}}^2 &= \|\hat{U}^{\text{rp}} - \tilde{U}^{\text{rp}} + \tilde{U}^{\text{rp}} - UO\|_{\text{F}}^2 \\ &\leq \|UO - \tilde{U}^{\text{rp}}\|_{\text{F}}^2 + \|\tilde{U}^{\text{rp}} - UO\|_{\text{F}}^2 \\ &= 2\|\tilde{U}^{\text{rp}} - UO\|_{\text{F}}^2, \end{aligned} \quad (\text{A.12})$$

where the first inequality follows from our assumption that \hat{U}^{rp} is the global solution minimum of the following k -means objective and UO is a feasible solution,

$$(\hat{\Theta}^{\text{rp}}, \hat{X}^{\text{rp}}) = \arg \min_{\Theta \in \mathbb{M}_{n,K}, X \in \mathbb{R}^{K \times K}} \|\Theta X - \tilde{U}^{\text{rp}}\|_{\text{F}}^2.$$

Then combine (A.12) with (A.11) and the bound of $\|\tilde{A}^{\text{rp}} - P\|_2$ in Theorem 1, we have with probability larger than $1 - n^{-s}$ that

$$\|\hat{U}^{\text{rp}} - UO\|_{\text{F}}^2 \leq \frac{c_1^2 16K n \alpha_n}{\gamma_n^2}. \quad (\text{A.13})$$

For notational convenience, we denote the right hand side of (A.13) as $\text{err}(K, n, c_1, \alpha_n, \gamma_n)$ in what follows.

Then, we proceed to bound the fraction of misclustered nodes. By Lemma 1, we can write $U = \Theta X$, where $\|X_{k*} - X_{l*}\|_2 = \sqrt{n_k^{-1} + n_l^{-1}}$ for all $1 \leq k < l \leq K$. Then $UO = \Theta XO = \Theta X'$ with $X' = XO$, and $\|X'_{k*} - X'_{l*}\|_2 = \sqrt{n_k^{-1} + n_l^{-1}}$ by the orthogonality

of O . Denote

$$\delta_k = \min_{l \neq k} \|X'_{k*} - X'_{l*}\|_2 = \sqrt{\frac{1}{n_k} + \frac{1}{\max\{n_l : l \neq k\}}}, \quad (\text{A.14})$$

and define

$$S_k = \{i \in G_k(\Theta) : \|(\hat{U})_{i*}^{\text{rp}} - (UO)_{i*}\|_{\text{F}} > \frac{\delta_k}{2}\}, \quad (\text{A.15})$$

where S_k is essentially the number of misclustered nodes in the true cluster k (after some permutation) as we will see soon. By the definition of S_k , it is easy to see

$$\sum_{k=1}^K |S_k| \delta_k^2 / 4 \leq \|\hat{U}^{\text{rp}} - UO\|_{\text{F}}^2 = \text{err}(K, n, c_1, \alpha_n, \gamma_n). \quad (\text{A.16})$$

Recall that $\delta_k = \min_{l \neq k} \|X'_{k*} - X'_{l*}\|_2 = \sqrt{\frac{1}{n_k} + \frac{1}{\max\{n_l : l \neq k\}}}$, then $n_k \delta_k^2 \geq 1$. Hence, (A.16) implies

$$\sum_{k=1}^K \frac{|S_k|}{n_k} \leq 4 \cdot \|\hat{U}^{\text{rp}} - UO\|_{\text{F}}^2 = 4 \cdot \text{err}(K, n, c_1, \alpha_n, \gamma_n). \quad (\text{A.17})$$

Next, we show that the nodes outside S_k are correctly clustered. Before that, we first prove $|S_k| < n_k$. We have by (A.16) that

$$|S_k| \leq \frac{4}{\delta_k^2} \text{err}(K, n, c_1, \alpha_n, \gamma_n). \quad (\text{A.18})$$

Since $n_k \delta_k^2 \geq 1$, it suffices to prove

$$4 \cdot \text{err}(K, n, c_1, \alpha_n, \gamma_n) < 1. \quad (\text{A.19})$$

which actually follows from the assumption (A2) by setting $c_2 = 1/64c_1^2$. As a result, we have $|S_k| < n_k$ for every $1 \leq k \leq K$. Therefore, $T_k \equiv G_k \setminus S_k \neq \emptyset$, where we recall that G_k denotes the nodes in the true cluster k . Let $T = \cup_{k=1}^K T_k$, we now show that the rows in $(UO)_{T*}$ has a one to one correspondence with those in \hat{U}_{T*}^{rp} . On the one hand, for $i \in T_k$

and $j \in T_l$ with $l \neq k$, $\hat{U}_{i^*}^{\text{rp}} \neq \hat{U}_{j^*}^{\text{rp}}$, otherwise we have the following contradiction

$$\begin{aligned}
\max\{\delta_k, \delta_l\} &\leq \|(UO)_{i^*} - (UO)_{j^*}\|_2 \\
&\leq \|(UO)_{i^*} - \hat{U}_{i^*}^{\text{rp}}\|_2 + \|(UO)_{j^*} - \hat{U}_{j^*}^{\text{rp}}\|_2 \\
&< \frac{\delta_k}{2} + \frac{\delta_l}{2},
\end{aligned} \tag{A.20}$$

where the first and last inequality follows from (A.14) and (A.15), respectively. On the other hand, for $i, j \in T_k$, $\hat{U}_{i^*}^{\text{rp}} = \hat{U}_{j^*}^{\text{rp}}$, because otherwise U_{T^*} has more than K distinct rows which contradicts the fact that the output cluster size is K .

Till now, we have proved the membership is correctly recovered outside of $\cup_{k=1}^K S_k$ and the rate of misclustered nodes in S_k is bounded as in (A.17). Therefore we obtain the claim of Theorem 2. \blacksquare

Proof of Theorem 3

We first bound the the derivation of $\tilde{B}_{ql}^{\text{rp}}$ from B_{ql} for each pair of $1 \leq q, l \leq K$, then we use the union bound to obtain a bound of $\|\tilde{B}^{\text{rp}} - B\|_\infty$. Denote \mathcal{E} be the event that (4.3) and (4.4) in Theorem 2 hold, then \mathcal{E} holds with probability larger than $1 - n^{-s}$ for any $s > 0$. In what follows, we derive the bound under the event \mathcal{E} .

Note that for any $1 \leq q, l \leq K$,

$$B_{ql} = \frac{\sum_{1 \leq i, j \leq n} P_{ij} \Theta_{iq} \Theta_{jl}}{\sum_{1 \leq i, j \leq n} \Theta_{iq} \Theta_{jl}}. \tag{A.21}$$

Then we have the following observations,

$$\begin{aligned}
& |\tilde{B}_{ql}^{\text{rp}} - B_{ql}| \\
&= \left| \frac{\sum_{1 \leq i, j \leq n} \tilde{A}_{ij}^{\text{rp}} \hat{\Theta}_{iq}^{\text{rp}} \hat{\Theta}_{jl}^{\text{rp}}}{\sum_{1 \leq i, j \leq n} \hat{\Theta}_{iq}^{\text{rp}} \hat{\Theta}_{jl}^{\text{rp}}} - \frac{\sum_{1 \leq i, j \leq n} P_{ij} \Theta_{iq} \Theta_{jl}}{\sum_{1 \leq i, j \leq n} \Theta_{iq} \Theta_{jl}} \right| \\
&\leq \left| \frac{\sum_{1 \leq i, j \leq n} \tilde{A}_{ij}^{\text{rp}} \hat{\Theta}_{iq}^{\text{rp}} \hat{\Theta}_{jl}^{\text{rp}}}{\sum_{1 \leq i, j \leq n} \hat{\Theta}_{iq}^{\text{rp}} \hat{\Theta}_{jl}^{\text{rp}}} - \frac{\sum_{1 \leq i, j \leq n} \tilde{A}_{ij}^{\text{rp}} \Theta_{iq} \Theta_{jl}}{\sum_{1 \leq i, j \leq n} \Theta_{iq} \Theta_{jl}} \right| + \left| \frac{\sum_{1 \leq i, j \leq n} \tilde{A}_{ij}^{\text{rp}} \Theta_{iq} \Theta_{jl}}{\sum_{1 \leq i, j \leq n} \Theta_{iq} \Theta_{jl}} - \frac{\sum_{1 \leq i, j \leq n} P_{ij} \Theta_{iq} \Theta_{jl}}{\sum_{1 \leq i, j \leq n} \Theta_{iq} \Theta_{jl}} \right| \\
&=: \mathcal{I}_1 + \mathcal{I}_2. \tag{A.22}
\end{aligned}$$

First, For \mathcal{I}_2 , we have

$$\begin{aligned}
\mathcal{I}_2 &\leq \frac{\|\tilde{A}^{\text{rp}} - P\|_{\text{F}} (\sum (\Theta_{iq} \Theta_{jl})^2)^{1/2}}{n_q n_l} = \frac{\|\tilde{A}^{\text{rp}} - P\|_{\text{F}}}{(n_q n_l)^{1/2}} \\
&\leq \frac{\sqrt{K+r} \|\tilde{A}^{\text{rp}} - P\|_2}{(n_q n_l)^{1/2}} \\
&\leq \frac{c_1 \sqrt{K+r} \sqrt{n \alpha_n}}{(n_q n_l)^{1/2}} \tag{A.23}
\end{aligned}$$

where the first inequality follows from the Cauchy-Schwarz's inequality and the fact that $\sum_{1 \leq i, j \leq n} \Theta_{iq} \Theta_{jl} = n_q n_l$, the second inequality follows from $\|A\|_{\text{F}} \leq \sqrt{\text{rank}(A)} \|A\|_2$ for any matrix A and the fact that $\tilde{A}^{\text{rp}} - P$ has rank at most $K+r$, and the last inequality is implied by the spectral bound of $\tilde{A}^{\text{rp}} - P$ (see (4.1)).

Next, we bound \mathcal{I}_1 . We have

$$\begin{aligned}
\mathcal{I}_1 &\leq \left| \frac{\sum_{1 \leq i, j \leq n} \tilde{A}_{ij}^{\text{rp}} \hat{\Theta}_{iq}^{\text{rp}} \hat{\Theta}_{jl}^{\text{rp}}}{\sum_{1 \leq i, j \leq n} \hat{\Theta}_{iq}^{\text{rp}} \hat{\Theta}_{jl}^{\text{rp}}} - \frac{\sum_{1 \leq i, j \leq n} \tilde{A}_{ij}^{\text{rp}} \Theta_{iq}^{\text{rp}} \Theta_{jl}^{\text{rp}}}{\sum_{1 \leq i, j \leq n} \hat{\Theta}_{iq}^{\text{rp}} \hat{\Theta}_{jl}^{\text{rp}}} \right| + \left| \frac{\sum_{1 \leq i, j \leq n} \tilde{A}_{ij}^{\text{rp}} \Theta_{iq}^{\text{rp}} \Theta_{jl}^{\text{rp}}}{\sum_{1 \leq i, j \leq n} \hat{\Theta}_{iq}^{\text{rp}} \hat{\Theta}_{jl}^{\text{rp}}} - \frac{\sum_{1 \leq i, j \leq n} \tilde{A}_{ij}^{\text{rp}} \Theta_{iq}^{\text{rp}} \Theta_{jl}^{\text{rp}}}{\sum_{1 \leq i, j \leq n} \Theta_{iq}^{\text{rp}} \Theta_{jl}^{\text{rp}}} \right| \\
&=: \mathcal{I}_{11} + \mathcal{I}_{12}. \tag{A.24}
\end{aligned}$$

For $1 \leq q \leq K$, denote the \hat{n}_q be the number of nodes in the q th estimated cluster, that

is, $\sum_i \tilde{\Theta}_{iq}^{\text{rp}} = \hat{n}_q$. Then we have for \mathcal{I}_{11} that,

$$\begin{aligned} \mathcal{I}_{11} &\leq \frac{1}{\hat{n}_q \hat{n}_l} \|\tilde{A}^{\text{rp}}\|_{\text{F}} \left(\sum_{i,j} (\Theta_{iq}^{\text{rp}} \Theta_{jl}^{\text{rp}} + \tilde{\Theta}_{iq}^{\text{rp}} \tilde{\Theta}_{jl}^{\text{rp}})^2 \right)^{1/2} \\ &\leq \frac{1}{\hat{n}_q \hat{n}_l} \|\tilde{A}^{\text{rp}}\|_{\text{F}} \left((n_q n_l)^{1/2} + (\hat{n}_q \hat{n}_l)^{1/2} \right) \\ &= \|\tilde{A}^{\text{rp}}\|_{\text{F}} \left(\frac{1}{(\hat{n}_q \hat{n}_l)^{1/2}} + \frac{(n_q n_l)^{1/2}}{\hat{n}_q \hat{n}_l} \right), \end{aligned} \quad (\text{A.25})$$

where the first and second inequality follows from the Cauchy-Schwarz's inequality and the triangle inequality, respectively. Using the Cauchy-Schwarz's inequality again, we have for \mathcal{I}_{12} that,

$$\mathcal{I}_{12} \leq \left| \sum_{ij} \tilde{A}_{ij}^{\text{rp}} \Theta_{iq}^{\text{rp}} \Theta_{jl}^{\text{rp}} \right| \frac{1}{n_q n_l} - \frac{1}{\hat{n}_q \hat{n}_l} \leq \|\tilde{A}^{\text{rp}}\|_{\text{F}} \left(\frac{1}{(n_q n_l)^{1/2}} + \frac{(n_q n_l)^{1/2}}{\hat{n}_q \hat{n}_l} \right). \quad (\text{A.26})$$

Putting (A.25) and (A.26) together, we have for \mathcal{I}_1 that,

$$\begin{aligned} \mathcal{I}_1 &\leq \|\tilde{A}^{\text{rp}}\|_{\text{F}} \left(\frac{1}{(n_q n_l)^{1/2}} + \frac{1}{(\hat{n}_q \hat{n}_l)^{1/2}} + 2 \frac{(n_q n_l)^{1/2}}{\hat{n}_q \hat{n}_l} \right) \\ &\leq (\|\tilde{A}^{\text{rp}} - P\|_{\text{F}} + \|P\|_{\text{F}}) \left(\frac{1}{(n_q n_l)^{1/2}} + \frac{1}{(\hat{n}_q \hat{n}_l)^{1/2}} + 2 \frac{(n_q n_l)^{1/2}}{\hat{n}_q \hat{n}_l} \right) \\ &\leq (c_1 \sqrt{K} + r \sqrt{n \alpha_n} + \sqrt{K} \delta_n) \left(\frac{1}{(n_q n_l)^{1/2}} + \frac{1}{(\hat{n}_q \hat{n}_l)^{1/2}} + 2 \frac{(n_q n_l)^{1/2}}{\hat{n}_q \hat{n}_l} \right), \end{aligned} \quad (\text{A.27})$$

where the last inequality is implied by $\|A\|_{\text{F}} \leq \sqrt{\text{rank}(A)} \|A\|_2$ for any matrix A and the following facts, $\tilde{A}^{\text{rp}} - P$ has rank at most $K + r$, P has rank K , the spectral bound of $\tilde{A}^{\text{rp}} - P$ (see (4.1)), and the largest eigenvalue of P is upper bounded by δ_n . To further bound (A.27), we now discuss the relationship between n_k and \hat{n}_k . Recall (4.3), we see that S_k is the number of misclustered nodes in the k th true cluster. Hence we have

$$\hat{n}_k \geq n_k - S_k \geq n_k - n_k c_2^{-1} \frac{K n \alpha_n}{\gamma_n^2} = n_k \left(1 - c_2^{-1} \frac{K n \alpha_n}{\gamma_n^2} \right), \quad (\text{A.28})$$

where the second inequality follows from (4.3), namely, the error bound for the sum of misclustering error over all K clusters. Combining (A.28) with (A.27) and using our as-

sumption that $n_k = n/K$ for any $1 \leq k \leq K$, we have the bound for \mathcal{I}_1 ,

$$\mathcal{I}_1 \leq (c_1\sqrt{K+r}\sqrt{n\alpha_n} + \sqrt{K}\delta_n)\left(\frac{K}{n} + \frac{K}{n}\left(1 - c_2^{-1}\frac{Kn\alpha_n}{\gamma_n^2}\right)^{-1} + \frac{2K}{n}\left(1 - c_2^{-1}\frac{Kn\alpha_n}{\gamma_n^2}\right)^{-2}\right). \quad (\text{A.29})$$

Consequently, combining (A.29) with (A.23), we have the following bound for $|\tilde{B}_{ql}^{\text{rp}} - B_{ql}|$,

$$|\tilde{B}_{ql}^{\text{rp}} - B_{ql}| \leq \left(\frac{2c_1\sqrt{K+r}K\sqrt{n\alpha_n}}{n} + \frac{\sqrt{K}K\delta_n}{n}\right)\left(1 + \left(1 - c_2^{-1}\frac{Kn\alpha_n}{\gamma_n^2}\right)^{-1} + 2\left(1 - c_2^{-1}\frac{Kn\alpha_n}{\gamma_n^2}\right)^{-2}\right). \quad (\text{A.30})$$

Finally, considering the event \mathcal{E} and using the union bound, we obtain the desired bound (4.14) for $\|\tilde{B}^{\text{rp}} - B\|_\infty$. \blacksquare

Proof of Theorem 4

Before deriving the spectral error bound of \tilde{A}^{rs} from P , we first give some notation. Recall that \tilde{A}^{rs} is obtained by two steps: (a) Randomly select each pair of the adjacency matrix A independently with probability p regardless of the value of A_{ij} , and for each pair (i, j) ($i < j$), the symmetric sparsified matrix \tilde{A}^{s} is defined as $\tilde{A}_{ij}^{\text{s}} = \frac{A_{ij}}{p}$ if (i, j) is selected, and $\tilde{A}_{ij}^{\text{s}} = 0$ otherwise, (b) Apply an iterative algorithm to find the nearly-optimal rank K approximation \tilde{A}^{rs} of \tilde{A}^{s} . Let G be the adjacency matrix of an Erdős-Renyi graph with each edge probability being $0 < p < 1$, then it is obvious that \tilde{A}_s in (a) can be written as $\tilde{A}_s = \frac{1}{p}G \circ A$. To simplify the proof, we assume that (b) finds the exactly optimal rank K approximation \tilde{A}^{rs} of \tilde{A}^{s} , i.e.,

$$\tilde{A}^{\text{rs}} = \arg \min_{\text{rank}(M) \leq K} \|\tilde{A}_s - M\|_2 = \arg \min_{\text{rank}(M) \leq K} \left\| \frac{1}{p}G \circ A - M \right\|_2. \quad (\text{A.31})$$

Now we proceed to derive the error bound of \tilde{A}^{rs} from P . Note that

$$\begin{aligned}
\|\tilde{A}^{\text{rs}} - P\|_2 &\leq \|\tilde{A}^{\text{rs}} - \frac{1}{p}G \circ A\|_2 + \|\frac{1}{p}G \circ A - P\|_2 \\
&\leq 2\|\frac{1}{p}G \circ A - P\|_2 = 2\|\frac{1}{p}G \circ (A - P) + \frac{1}{p}G \circ P - P\|_2 \\
&\leq 2\|\frac{1}{p}G \circ (A - P)\|_2 + 2\|\frac{1}{p}G \circ P - P\|_2, \\
&= \mathcal{I}_1 + \mathcal{I}_2,
\end{aligned} \tag{A.32}$$

where the second inequality follows from (A.31) and the fact that $\text{rank}(P) = K$. Next we bound \mathcal{I}_1 and \mathcal{I}_2 , respectively.

To bound \mathcal{I}_1 , we need the following results on the spectral-norm bound of a random matrix with independent and bounded entries (see Proposition 13 of Klopp (2015); Lemma 3 of Li et al. (2016)).

Proposition 1 *Let X be an $n \times n$ random matrix with each entry X_{ij} being independent and bounded such that $\max_{ij}|X_{ij}| \leq \sigma$. Then for any $\nu > 0$, there exists constant $c_6 = c_6(\sigma, \nu) > 0$ such that,*

$$\|X\|_2 \leq c_6 \max(\sigma_1, \sigma_2, \sqrt{\log n}), \tag{A.33}$$

with probability larger than $1 - n^{-\nu}$, where

$$\sigma_1 = \max_i \sqrt{\mathbb{E} \sum_j X_{ij}^2} \quad \text{and} \quad \sigma_2 = \max_j \sqrt{\mathbb{E} \sum_i X_{ij}^2}. \tag{A.34}$$

We now bound $\mathcal{I}_1 = 2\|\frac{1}{p}G \circ (A - P)\|_2$ using Proposition 1 by conditioning on $A - P \equiv W$. We have $(G \circ W)_{ij} = b_{ij}W_{ij}$, where $b_{ij} \sim \text{Bernoulli}(p)$. And we also have,

$$\begin{aligned}
\sigma_1 &= \max_i \sqrt{\mathbb{E}(\sum_j b_{ij}^2 W_{ij}^2 | W)} = \max_i \sqrt{\sum_j W_{ij}^2 \mathbb{E}(b_{ij}^2 | W)} \\
&= \max_i \sqrt{p} \sqrt{\|W_{i*}\|_2^2} = \sqrt{p} \sqrt{\|W\|_{2,\infty}^2} \leq \sqrt{p} \|W\|_2,
\end{aligned} \tag{A.35}$$

where the last inequality follows from the fact that $\|W\|_{2,\infty} \leq \|W\|_2$. In a similar way, (A.35) holds for σ_2 . Therefore, by Proposition 1, we have with probability $1 - n^{-\nu}$ that,

$$\mathcal{I}_1 = 2\left\|\frac{1}{p}G \circ (A - P)\right\|_2 = \frac{2}{p}\|G \circ W\| \leq \frac{2}{p}c_6 \max(\sqrt{p}\|W\|_2, \sqrt{\log n}), \quad (\text{A.36})$$

where c_6 depends on $\sigma = 1$ and ν . To further bound \mathcal{I}_1 , we use the following spectral norm error bound of $A - P$ proved in Lei and Rinaldo (2015). That is, under assumption (A1),

$$\|W\|_2 = \|A - P\|_2 \leq c_7\sqrt{n\alpha_n}, \quad (\text{A.37})$$

with probability larger than $1 - n^{-\nu}$, where c_7 depends on ν and c_0 , and we set ν to be identical to that in (A.36). As a result, under the assumption (A1), we have with probability larger than $1 - 2n^{-\nu}$ that,

$$\mathcal{I}_1 \leq c_8 \max\left(\sqrt{\frac{n\alpha_n}{p}}, \frac{\sqrt{\log n}}{p}\right), \quad (\text{A.38})$$

where $c_8 = 2c_6 \cdot \max(c_7, 1)$.

Next, we proceed to bound \mathcal{I}_2 . We will use the following bound on the spectral derivation of a random matrix from its expectation, which corresponds to Corollary 4 and Theorem 5 in Gittens and Tropp (2009).

Proposition 2 *Suppose B is a fixed matrix, and let X be a random matrix with each entry X_{jk} being independent and bounded such that $\max_{jk}|X_{jk}| \leq \frac{D}{2}$ almost surely, for which $\mathbb{E}(X) = B$. Then for all $\delta > 0$,*

$$\|X - B\|_2 \leq (1 + \delta)\mathbb{E}\|B - X\|_2, \quad (\text{A.39})$$

with probability larger than $1 - \exp^{-\delta^2(\mathbb{E}\|X - B\|_2)^2/4D^2}$. And

$$\mathbb{E}\|X - B\|_2 \leq c_9 \left(\max_j \left(\sum_k \text{Var}(X_{jk}) \right)^{1/2} + \max_k \left(\sum_j \text{Var}(X_{jk}) \right)^{1/2} + \left(\sum_{jk} \mathbb{E}(X_{jk} - b_{jk})^4 \right)^{1/4} \right). \quad (\text{A.40})$$

In our case, $B := P$ and $X := \frac{1}{p}G \circ P$. Write

$$X_{jk} = \frac{P_{jk}}{p} \text{Bernoulli}(p),$$

then it is obvious that $\mathbb{E}(X) = B$, and $\max_{jk} |X_{jk}| \leq \alpha_n/p$. And we have $\text{Var}X_{jk} \leq P_{jk}^2/p$ and

$$\mathbb{E}(X_{jk} - P_{jk})^4 \leq \text{Var}X_{jk} \cdot \|X_{jk} - P_{jk}\|_\infty^2 \leq \frac{P_{jk}^2}{p} \cdot \max\left(P_{jk}, \frac{P_{jk}}{p} - P_{jk}\right)^2 = \frac{P_{jk}^4}{p} \cdot \max\left(1, \left(\frac{1}{p} - 1\right)\right)^2. \quad (\text{A.41})$$

Hence, by (A.40) and noting that $P_{ij} \leq \alpha_n$, we have

$$\begin{aligned} \mathcal{I}_2 &= 2\|X - P\|_2 \\ &\leq 2c_9 \left(2\alpha_n \sqrt{\frac{n}{p}} + \alpha_n \frac{\sqrt{n}}{p^{1/4}} \max\left(1, \sqrt{\frac{1}{p} - 1}\right) \right) \\ &\leq c_{10} \sqrt{\frac{n\alpha_n^2}{p}} \left(1 + p^{1/4} \cdot \max\left(1, \sqrt{\frac{1}{p} - 1}\right) \right), \end{aligned} \quad (\text{A.42})$$

where $c_{10} = 4c_9$, and (A.42) holds with probability larger than $1 - \exp\left(-c_4 np(1 + p^{1/4} \cdot \max\left(1, \sqrt{\frac{1}{p} - 1}\right)^2)\right)$.

Consequently, combining (A.38) with (A.42), we have with probability larger than $1 - 2n^{-\nu} - \exp\left(-c_4 np(1 + p^{1/4} \cdot \max\left(1, \sqrt{\frac{1}{p} - 1}\right)^2)\right)$ that

$$\begin{aligned} \|\tilde{A}^{\text{rs}} - P\|_2 &= \mathcal{I}_1 + \mathcal{I}_2 \\ &\leq c_3 \max\left(\sqrt{\frac{n\alpha_n}{p}}, \frac{\sqrt{\log n}}{p}, \sqrt{\frac{n\alpha_n^2}{p}} \left(1 + p^{1/4} \cdot \max\left(1, \sqrt{\frac{1}{p} - 1}\right)\right)\right), \end{aligned} \quad (\text{A.43})$$

where $c_3 = \max\{2c_8, 2c_{10}\}$. The conclusion in Theorem 4 is arrived. \blacksquare

References

- Abbe, E. (2018). Community detection and stochastic block models: recent developments. *The Journal of Machine Learning Research* 18(1), 6446–6531.
- Abbe, E., J. Fan, K. Wang, and Y. Zhong (2019). Entrywise eigenvector analysis of random matrices with low expected rank. *Annals of Statistics*, preprint.
- Achlioptas, D. and F. McSherry (2007). Fast computation of low-rank matrix approximations. *Journal of the ACM (JACM)* 54(2), 1–19.
- Adamic, L. A. and N. Glance (2005). The political blogosphere and the 2004 us election: divided they blog. In *Proceedings of the 3rd international workshop on Link discovery*, pp. 36–43. ACM.
- Ahn, K., K. Lee, and C. Suh (2018). Hypergraph spectral clustering in the weighted stochastic block model. *IEEE Journal of Selected Topics in Signal Processing* 12(5), 959–974.
- Allen-Zhu, Z. and Y. Li (2016). Lazysvd: even faster svd decomposition yet without agonizing pain. In *Advances in Neural Information Processing Systems*, pp. 974–982.
- Arora, S., E. Hazan, and S. Kale (2006). A fast random sampling algorithm for sparsifying matrices. In *Approximation, Randomization, and Combinatorial Optimization. Algorithms and Techniques*, pp. 272–279. Springer.
- Baglama, J. and L. Reichel (2005). Augmented implicitly restarted lanczos bidiagonalization methods. *SIAM Journal on Scientific Computing* 27(1), 19–42.
- Bhatia, R. (1997). Graduate texts in mathematics: Matrix analysis.
- Chin, P., A. Rao, and V. Vu (2015). Stochastic block model and community detection in sparse graphs: A spectral algorithm with optimal rate of recovery. In *Conference on Learning Theory*, pp. 391–423.

- Choi, D. S., P. J. Wolfe, and E. M. Airoldi (2012). Stochastic blockmodels with a growing number of classes. *Biometrika* 99(2), 273–284.
- Davis, C. and W. M. Kahan (1970). The rotation of eigenvectors by a perturbation. iii. *SIAM Journal on Numerical Analysis* 7(1), 1–46.
- Drineas, P., M. Magdon-Ismail, M. W. Mahoney, and D. P. Woodruff (2012). Fast approximation of matrix coherence and statistical leverage. *Journal of Machine Learning Research* 13(Dec), 3475–3506.
- Drineas, P. and M. W. Mahoney (2016). Randnla: randomized numerical linear algebra. *Communications of the ACM* 59(6), 80–90.
- Drineas, P., M. W. Mahoney, and S. Muthukrishnan (2006). Sampling algorithms for l_2 regression and applications. In *Proceedings of the seventeenth annual ACM-SIAM symposium on Discrete algorithm*, pp. 1127–1136. Society for Industrial and Applied Mathematics.
- Drineas, P., M. W. Mahoney, S. Muthukrishnan, and T. Sarlós (2011). Faster least squares approximation. *Numerische mathematik* 117(2), 219–249.
- Erichson, N. B., S. Voronin, S. L. Brunton, and J. N. Kutz (2019). Randomized matrix decompositions using r . *Journal of Statistical Software* 89(1), 1–48.
- Gao, C., Z. Ma, A. Y. Zhang, and H. H. Zhou (2017). Achieving optimal misclassification proportion in stochastic block models. *The Journal of Machine Learning Research* 18(1), 1980–2024.
- Gittens, A. and J. A. Tropp (2009). Error bounds for random matrix approximation schemes. *arXiv preprint arXiv:0911.4108*.
- Goldenberg, A., A. X. Zheng, S. E. Fienberg, E. M. Airoldi, et al. (2010). A survey of statistical network models. *Foundations and Trends® in Machine Learning* 2(2), 129–233.

- Halko, N., P.-G. Martinsson, and J. A. Tropp (2011). Finding structure with randomness: Probabilistic algorithms for constructing approximate matrix decompositions. *SIAM review* 53(2), 217–288.
- Holland, P. W., K. B. Laskey, and S. Leinhardt (1983). Stochastic blockmodels: First steps. *Social networks* 5(2), 109–137.
- Ji, P. and J. Jin (2016). Coauthorship and citation networks for statisticians. *The Annals of Applied Statistics* 10(4), 1779–1812.
- Joseph, A. and B. Yu (2016). Impact of regularization on spectral clustering. *The Annals of Statistics* 44(4), 1765–1791.
- Klopp, O. (2015). Matrix completion by singular value thresholding: sharp bounds. *Electronic journal of statistics* 9(2), 2348–2369.
- Kolaczyk, E. D. (2009). In *Statistical Analysis of Network Data: Methods and Models*. Springer.
- Kumar, A., Y. Sabharwal, and S. Sen (2004). A simple linear time $(1 + \epsilon)$ -approximation algorithm for k-means clustering in any dimensions. In *Annual Symposium on Foundations of Computer Science*, Volume 45, pp. 454–462. IEEE COMPUTER SOCIETY PRESS.
- Lehoucq, R. B. (1995). Analysis and implementation of an implicitly restarted arnoldi iteration. Technical report, RICE UNIV HOUSTON TX DEPT OF COMPUTATIONAL AND APPLIED MATHEMATICS.
- Lei, J. and A. Rinaldo (2015). Consistency of spectral clustering in stochastic block models. *The Annals of Statistics* 43(1), 215–237.
- Leskovec, J., J. Kleinberg, and C. Faloutsos (2007). Graph evolution: Densification and shrinking diameters. *ACM Transactions on Knowledge Discovery from Data (TKDD)* 1(1), 1–40.

- Li, M. and E. L. Kang (2019). Randomized algorithms of maximum likelihood estimation with spatial autoregressive models for large-scale networks. *Statistics and Computing* 29(5), 1165–1179.
- Li, T., E. Levina, and J. Zhu (2016). Network cross-validation by edge sampling. *arXiv preprint arXiv:1612.04717*.
- Ma, P., M. W. Mahoney, and B. Yu (2015). A statistical perspective on algorithmic leveraging. *The Journal of Machine Learning Research* 16(1), 861–911.
- Mahoney, M. W. (2011). Randomized algorithms for matrices and data. *Foundations and Trends® in Machine Learning* 3(2), 123–224.
- Mahoney, M. W. and P. Drineas (2009). Cur matrix decompositions for improved data analysis. *Proceedings of the National Academy of Sciences* 106(3), 697–702.
- Manning, C., P. Raghavan, and H. Schütze (2010). Introduction to information retrieval. *Natural Language Engineering* 16(1), 100–103.
- Martinsson, P.-G. (2016). Randomized methods for matrix computations. *arXiv preprint arXiv:1607.01649*.
- Matoušek, J. (2000). On approximate geometric k-clustering. *Discrete & Computational Geometry* 24(1), 61–84.
- Newman, M. (2018). *Networks*. Oxford university press.
- Pilanci, M. and M. J. Wainwright (2016). Iterative hessian sketch: Fast and accurate solution approximation for constrained least-squares. *The Journal of Machine Learning Research* 17(1), 1842–1879.
- Pilanci, M. and M. J. Wainwright (2017). Newton sketch: A near linear-time optimization algorithm with linear-quadratic convergence. *SIAM Journal on Optimization* 27(1), 205–245.

- Qin, T. and K. Rohe (2013). Regularized spectral clustering under the degree-corrected stochastic blockmodel. In *Advances in Neural Information Processing Systems*, pp. 3120–3128.
- Raskutti, G. and M. W. Mahoney (2016). A statistical perspective on randomized sketching for ordinary least-squares. *The Journal of Machine Learning Research* 17(1), 7508–7538.
- Rohe, K., S. Chatterjee, and B. Yu (2011). Spectral clustering and the high-dimensional stochastic block model. *The Annals of Statistics* 39(4), 1878–1915.
- Sarkar, P., P. J. Bickel, et al. (2015). Role of normalization in spectral clustering for stochastic blockmodels. *The Annals of Statistics* 43(3), 962–990.
- Spielman, D. A. and N. Srivastava (2011). Graph sparsification by effective resistances. *SIAM Journal on Computing* 40(6), 1913–1926.
- Su, L., W. Wang, and Y. Zhang (2017). Strong consistency of spectral clustering for stochastic block models. *arXiv preprint arXiv:1710.06191*.
- Von Luxburg, U. (2007). A tutorial on spectral clustering. *Statistics and Computing* 17(4), 395–416.
- Vu, V. Q. and J. Lei (2013). Minimax sparse principal subspace estimation in high dimensions. *The Annals of Statistics* 41(6), 2905–2947.
- Wang, H. (2018). More efficient estimation for logistic regression with optimal subsample. *arXiv preprint arXiv:1802.02698*.
- Wang, H., M. Yang, and J. Stufken (2019). Information-based optimal subdata selection for big data linear regression. *Journal of the American Statistical Association* 114(525), 393–405.
- Wang, H., R. Zhu, and P. Ma (2018). Optimal subsampling for large sample logistic regression. *Journal of the American Statistical Association* 113(522), 829–844.

- Wang, S., A. Gittens, and M. W. Mahoney (2017). Sketched ridge regression: Optimization perspective, statistical perspective, and model averaging. *The Journal of Machine Learning Research* 18(1), 8039–8088.
- Witten, R. and E. Candès (2015). Randomized algorithms for low-rank matrix factorizations: sharp performance bounds. *Algorithmica* 72(1), 264–281.
- Xia, D. and M. Yuan (2019). Statistical inferences of linear forms for noisy matrix completion. *arXiv preprint arXiv:1909.00116*.
- Yin, H., A. R. Benson, J. Leskovec, and D. F. Gleich (2017). Local higher-order graph clustering. In *Proceedings of the 23rd ACM SIGKDD International Conference on Knowledge Discovery and Data Mining*, pp. 555–564. ACM.
- Yun, S.-Y. and A. Proutiere (2014). Accurate community detection in the stochastic block model via spectral algorithms. *arXiv preprint arXiv:1412.7335*.
- Yun, S.-Y. and A. Proutiere (2016). Optimal cluster recovery in the labeled stochastic block model. In *Advances in Neural Information Processing Systems*, pp. 965–973.
- Zhou, J., Y. Tu, Y. Chen, and H. Wang (2017). Estimating spatial autocorrelation with sampled network data. *Journal of Business & Economic Statistics* 35(1), 130–138.